HHS Public Access

Author manuscript

Med Phys. Author manuscript; available in PMC 2024 July 08.

Published in final edited form as:

Med Phys. 2023 August ; 50(8): e865–e903. doi:10.1002/mp.16536.

Use of Electronic Portal Imaging Devices for Pre-Treatment and *in vivo* Dosimetry Patient-Specific IMRT and VMAT QA: Report of AAPM Task Group 307

Nesrin Dogan, PhD[1], **Ben J. Mijnheer, PhD**[2], **Kyle Padgett, PhD**[1], **Adrian Nalichowski, PhD**[3], **Chuan Wu, PhD**[4], **Matthew J. Nyflot, PhD**[5], **Arthur J. Olch, PhD**[6], **Niko Papanikolaou, PhD, MBA**[7], **Jie Shi, PhD**[8], **Shannon M. Holmes, PhD**[9], **Jean Moran, PhD**[10], **Peter B. Greer, PhD**[11,12]

[1]Department of Radiation Oncology, University of Miami, Miami, FL

[2]Department of Radiation Oncology, Netherlands Cancer Institute, Amsterdam, Netherlands

[3]Department of Radiation Oncology, Karmanos Cancer Institute, Detroit, MI

[4]Department of Radiation Oncology, Sutter Medical Foundation, Roseville, CA

[5]Department of Radiation Oncology, University of Washington, Seattle, WA

[6]Department of Radiation Oncology, University of Southern California, and Children's Hospital Los Angeles, Los Angeles, CA

[7]Department of Radiation Oncology, University of Texas SA, San Antonio, TX

[8]Sun Nuclear Corporation, Melbourne, FL

[9]Standard Imaging, Middleton, WI

[10]Department of Radiation Oncology, Memorial Sloan Kettering Cancer Center, New York, NY

[11]Department of Radiation Oncology, Calvary Mater Newcastle, and University of Newcastle, Newcastle, Australia

[12]School of Information and Physical Sciences, University of Newcastle, Newcastle, Australia

Abstract

Purpose: Electronic Portal Imaging Devices (EPIDs) have been widely utilized for Patient-Specific QA (PSQA) and their use for transit dosimetry applications is emerging. Yet there are no specific guidelines on the potential uses, limitations, and correct utilization of EPIDs for these purposes. The AAPM Task Group 307 (TG307) provides a comprehensive review of the physics, modeling, algorithms and clinical experience with EPID-based pre-treatment and transit dosimetry techniques. This review also includes the limitations and challenges in the clinical implementation

DISCLOSURE STATEMENT

The members of AAPM TG-307 listed below disclose the following potential Conflict(s) of Interest related to subject matter or materials presented in this document.

Jie Shi, PhD, works for Sun Nuclear Corporation (A Mirion Medical Company), and Shannon M. Holmes, PhD, works for Standard Imaging, whose EPID software products, are discussed in this work.

The rest of the authors have no conflict of interest related to subject matter or materials presented in this document.

of EPIDs, including recommendations for commissioning, calibration and validation, routine QA, tolerance levels for gamma analysis and risk-based analysis.

Methods: Characteristics of the currently available EPID systems and EPID-based PSQA techniques are reviewed. The details of the physics, modeling, and algorithms for both Pre-treatment and Transit dosimetry methods are discussed, including clinical experience with different EPID dosimetry systems. Commissioning, calibration, and validation, tolerance levels and recommended tests, are reviewed, and analyzed. Risk-based analysis for EPID dosimetry is also addressed.

Results: Clinical experience, commissioning methods and tolerances for EPID-based PSQA system are described for pre-treatment and transit dosimetry applications. The sensitivity, specificity, and clinical results for EPID dosimetry techniques are presented as well as examples of patient-related and machine-related error detection by these dosimetry solutions. Limitations and challenges in clinical implementation of EPIDs for dosimetric purposes are discussed and acceptance and rejection criteria are outlined. Potential causes of and evaluations of pre-treatment and transit dosimetry failures are discussed. Guidelines and recommendations developed in this report are based on the extensive published data on EPID QA along with the clinical experience of the TG307 members. Conclusion: TG307 focused on the commercially available EPID-based dosimetric tools and provides guidance for medical physicists in the clinical implementation of EPID-based patient-specific pre-treatment and transit dosimetry QA solutions including IMRT and VMAT treatments.

1 INTRODUCTION

1.1 Background and Rationale

The clinical use of electronic portal imaging devices (EPIDs) began in the 1990s, and EPIDs became the standard onboard imaging devices on all modern linear accelerators (linacs) in the early 2000s (Antonuk, Yorkston et al. 1996, Antonuk, Boudry et al. 1993). EPIDs have been utilized mainly for verification of patient positioning by generating radiographs of the patient just before or during treatment delivery. The American Association of Physicists in Medicine (AAPM) Task Group (TG) Report 58 (TG-58) on Clinical Use of Electronic Portal Imaging published in 2001 provided necessary information to implement EPIDs for clinical use, which included the comprehensive review of physics of portal imaging, different portal imaging technology such as camera-based and matrix ion chamber (IC)-based EPIDs, commissioning and quality assurance (QA), and detailed steps for successful clinical implementation for patient setup verification (Herman, Balter et al. 2001). The TG-58 indicated the lack of widespread clinical applications and underutilization of EPIDs in the U.S. mainly due to inferior image quality. However, EPIDs were still used because they provide quantitative data and online feedback compared with film. The report also briefly mentioned the potential use of EPIDs for advanced applications without going into any detail, including treatment QA (Luchka, Chen et al. 1996), *in vivo* dosimetry (IVD) measurements during treatment delivery (Kirby and Williams 1995, Essers, Boellaard et al. 1996), and verification for advanced treatment delivery techniques such as intensity modulated radiation therapy (IMRT). Furthermore, users were cautioned against using

EPIDs for dose measurement due to significant uncertainties related to modeling and calibration.

Since the publication of TG-58, there has been widespread implementation of sophisticated treatment delivery techniques such as IMRT, volumetric modulated arc therapy (VMAT), and adaptive radiotherapy (ART). Hence, the demand for reliable patient-specific QA (PSQA) tools has dramatically increased (Masi, Casamassima et al. 2011, Hussein, Adams et al. 2013, Son, Baek et al. 2015, Colodro, Berna et al. 2017). During the last decade, many new commercial dosimetry tools, and techniques (both hardware and software) have become available for PSQA, replacing more cumbersome film and ionization chamber measurements (Childress, Salehpour et al. 2005). Current IMRT and VMAT QA methods which use non-EPID-based QA devices, such as two-dimensional (2D) diode and IC arrays, have several inherent limitations such as reduced density of measurement points, reduced efficiency, and lesser ease of use compared with EPID (Kausar, Mani et al. 2019, Olaciregui-Ruiz, Vivas-Maiques et al. 2019).

Shortly after the introduction of EPIDs for patient positioning, several groups investigated the dosimetric characteristics of different EPID designs for possible use for pretreatment IMRT QA since EPID images can also contain dose information. Both pretreatment and IVD IMRT and VMAT QA methods have been a strong research interest since the introduction of amorphous silicon (a-Si) flat-panel technology and have been described in detail in many publications (van Etmpt, McDermott et al. 2008, Greer, Fuangrod et al. 2013, Mijnheer, González et al. 2015, Mijnheer, Jomehzadeh et al. 2018). EPIDs can be utilized in a variety of different ways as radiation dosimeters, including linac QA, pretreatment patient QA, and three-dimensional (3D) estimation of dose in patient as an *in vivo* dosimeter (Van Esch, Depuydt et al. 2004, Rowshanfarzad, McGarry et al. 2014, Cilla, Meluccio et al. 2016). With the introduction of current a-Si flat-panel EPID technology, which generates better image quality and demonstrates more useful dosimetric characteristics, they are now routinely utilized for pretreatment QA (PTQA) and transit (*in vivo*) dosimetry measurements in an increasing number of clinics (Mijnheer 2017[a]).

Commercial EPID dosimetry software products are available from several vendors, including two linac manufacturers. However, there are currently no specific guidelines for clinical physicists on the potential uses and limitations and correct utilization of EPID dosimetry, as well as the clinical implementation of EPIDs as a PSQA tool. The goal of this TG-307 is to provide a resource for medical physicists who will commission and implement EPID-based PSQA tools. The EPID systems discussed in this report refer to the combination of EPID imaging system and software used to analyze images dosimetrically, unless otherwise stated. The charges of the TG-307 are given below:

1. to provide a discussion on limitations and clinical applications of commercially available EPIDs;
2. to provide a review and assessment of the current IMRT/VMAT QA methods utilizing EPIDs — specifically providing a discussion on the challenges in clinical implementation of EPIDs;
3. to recommend tests to evaluate an EPID-based QA system; and

4. to provide recommendations for the correct utilization and guidelines on the clinical implementation of EPIDs for the PSQA of IMRT/VMAT as a PTQA tool (before treatment) and transit dosimetry tool (during treatment).

The goal of the proposed TG-307 report is to provide a discussion on the charges included above. In this report, physics, modeling and algorithms, and clinical experience with EPID-based pretreatment and transit dosimetry techniques, including limitations and challenges in clinical implementation of EPIDs, are reviewed and discussed in detail. Clinical implementation of EPID systems is presented, including recommendations for commissioning, calibration and validation, routine QA, and tolerance levels for gamma (γ) analysis. Recommendation on risk-based analysis for EPID dosimetry is also briefly discussed. A summary of current EPID technology and the EPID dosimetry products are shown in Table 1. Other applications of EPIDs, such as utilization of EPID panels and other onboard imaging systems for acceptance testing, monthly QA, and daily QA of linacs, are outside of the scope of this report.

1.2 Nomenclature and Definitions

In this section, we will start by defining several concepts and procedures used in this report for EPID-based PSQA of IMRT and VMAT. These are partly based on the definitions found in the European Society for Radiotherapy and Oncology (ESTRO) paper titled “IVD in EBRT: Requirements and Future Directions for Research, Development and Clinical Practice” (Olaciregui-Ruiz, Beddar et al. 2020).

PSQA includes but is not limited to pretreatment measurement QA and transit dosimetry.

Pretreatment measurement QA: before patient treatment, measurements are performed to confirm the deliverability and quality of the patient plan.

Non-transit dosimetry is a determination of the dose in the detector/patient/phantom without any attenuating medium, e.g., a determination of the incident energy fluence, such as for PTQA.

Transit dosimetry is a dose measurement when treatment beams have passed through a patient, i.e., IVD, or phantom before being measured by a detector.

IVD as used in this report is a radiation measurement that (i) is acquired while the patient is treated, (ii) contains information on the position of the patient with respect to the treatment dose distribution, and (iii) contains information related to the absorbed dose in the patient. This definition implies that an IVD system must be able to capture errors due to treatment delivery device, dose calculation, patient position, and patient anatomy changes.

Relative transit delivery monitoring: with this methodology, an initial measurement is made with a patient and used as a reference for all subsequent checks without converting the image to dose. Such a comparison of an EPID image made during a specific fraction of a patient treatment with a reference EPID image may miss dose errors present in the reference image and therefore is limited solely to a constancy check and is not an IVD measurement.

2 OVERVIEW AND UTILIZATION OF EPIDs

A variety of different EPID technologies with different designs have been commercially available for patient portal imaging. The first generation of EPIDs included the scanning liquid ionization chamber array, Portal Vision (Varian Medical Systems, Palo Alto, CA), charge-coupled device (CCD) cameras (SRI-100, Elekta Medical Systems, Stockholm, Sweden), and camera-based systems (Beam View Plus, Siemens Healthcare). The scanning liquid ionization chamber array based EPID was originally developed at the Netherlands Cancer Institute (Meertens, van Herk et al. 1985) and later became commercially available as Portal Vision. Several camera-based EPIDs were developed and commercialized, and details of these systems were published by many investigators (Heijmen, Pasma et al. 1995, Glendinning and Bonnett 2000, Nijsten, Minken et al. 2004). These devices had limited dosimetric capability and produced poor quality images. The dosimetric characteristics of the first generation of EPIDs were summarized in several publications (Kirby and Glendinning 2006, van Elmpt, McDermott et al. 2008). The second generation of EPIDs included active matrix flat-panel imagers. These were initially developed at the University of Michigan and were later offered by all linac manufacturers due to the enhanced image quality and potential for dosimetric use (Herman, Balter et al. 2001, Kirby and Glendinning 2006).

Current EPID technology based on a-Si flat-panels was introduced in the early 2000s and is now standard on modern linacs. a-Si EPIDs produce much higher quality images and have improved dosimetric characteristics compared with older types of EPIDs (McCurdy and Greer 2009, Antonuk 2016). They were first described by Antonuk et al. (Antonuk, Yorkston et al. 1995) and have been the focus of many dosimetric investigations (Siebers, Kim et al. 2004, Greer, Cadman et al. 2009, Gustafsson, Vial et al. 2011). A detailed technical overview of various EPID-based dosimetric technologies, including a-Si EPIDs, was included in the EPID dosimetry review article by van Elmpt et al. (van Elmpt, McDermott et al. 2008). A more recent review includes more than 100 papers since the publication of the van Elmpt et al. 2008 review (McCurdy, Greer, Bedford 2017). Briefly, the main operational characteristics of the major currently available EPID systems are described in Table 2 below.

The main components of an a-Si EPID are shown in Figure 1. Incident x-rays interact in the copper buildup layer and phosphor scintillator layer producing visible photons that are detected by the photodiode array. A small percentage of the photodiode signal is from direct x-ray interactions in the array. The resulting image represents the energy absorbed in the photodiode array from the incident energy fluence of the beam. X-ray and light scatter within the EPID layers also result in a “spreading” of the incident fluence characterized by the point spread function of the detector. The measured signal is in many cases very different to dose measured in water or with a water-equivalent 2D array detector due to both response and scattering differences. The dose-response characteristics of the three commercially available a-Si flat-panel EPIDs have been described in detail in several publications (McDermott, Louwe et al. 2004, Parent, Fielding et al. 2007). Issues specific to a-Si EPIDs, including overresponse to low energies, imager size limitation, ghosting, and image lag, were also reported by many investigators (McCurdy, Luchka et al. 2001,

McDermott, Nijsten et al. 2006, Greer 2007). Advances in EPID technology, including high uniformity, linearity, higher resolution, and faster readout, have made significant improvements in the potential of EPIDs as dosimeters (Greer and Vial 2011, Mijnheer, Olaciregui-Ruiz et al. 2013, McCurdy, Greer, and Bedford 2017).

There are several novel applications for EPID utilization that are currently being employed or in development. Some of these applications, covered in this TG report, improve upon the PTQA process by using in-air EPID measurements along with a planning computed tomography (CT) to calculate 2D dose in phantom and 3D dose distributions in the patient and use dose-volume histograms (DVHs) to provide more clinically insightful analysis. The DVH analysis approach may detect issues with the treatment plan that can significantly impact planning target volume (PTV) coverage or potential organ at risk (OAR) constraint failure, i.e., these analyses may be more impactful and meaningful than current methods, which lack a straightforward connection between QA metrics and plan quality (Nelms, Opp et al. 2012, Olaciregui-Ruiz, Rozendaal et al. 2017). Another utilization of EPID panels is transit dosimetry applications. Much of the anatomy can change in both size and location throughout the course of treatment and can dosimetrically impact both target coverage and OARs. IVD, along with daily 3D imaging, has the potential to reconstruct 3D dose distributions in daily anatomy, giving powerful insight into the daily and cumulative dosimetric impacts of these anatomical changes (Rozendaal, Mijnheer et al. 2015). Many of the applications reviewed in our report use EPIDs to improve upon existing QA procedures by utilizing some inherent optimal properties of these systems, namely, the digital nature of the data, the fact that the EPID is integrated into the radiation delivery system equipment, and potential for the automation of analysis.

2.1 EPID-based Patient-Specific QA Techniques

The various EPID dosimetry approaches have been described comprehensively in a review article by van Elmpt et al. (van Elmpt, McDermott et al. 2008) and have been discussed further in the more recent literature review by McCurdy et al. (McCurdy, Greer, and Bedford 2017). They are schematically represented in Figure 2. Information about the dose calculation algorithms used in these models is provided in Section 3.

Dose or image comparisons can be made at the EPID level (in a virtual slab phantom) or in the patient/phantom using a forward or back-projection approach, respectively. Non-transit forward methods compare measured images or 2D dose distributions with predicted images or 2D dose distributions at the EPID level (Figure 2a). In the image prediction and comparison approach, a separate algorithm is used to calculate the predicted image, and the TPS model is not used. In the alternative forward non-transit method, the measured image is converted to a dose at the EPID level. This 2D dose distribution can then be compared with the dose distribution calculated by the TPS. Many of the commercial EPID dosimetry systems calculate the reference dose in water from the exported patient plan using their own algorithms. For non-transit dosimetry, the distinction between forward- and back-projection is less distinct than transit dosimetry. As there is usually no phantom or patient present, the EPID for some systems can be positioned at the isocenter level. To maintain consistency with previous definitions, we have classified the methods according to Figure 2 and included

all methods that do not back-project a fluence and calculate dose in the patient CT dataset or 3D phantom as forward methods.

In the transit dosimetry forward approach (Figure 2b), grayscale distributions measured with the EPID are compared directly or after conversion to dose values with predicted grayscale or dose distributions. This method is also used for relative transit delivery monitoring, in which an initial measurement is made with a patient present and used as a reference for subsequent checks.

In the non-transit dosimetry back-projection approach (Figure 2c), the photon fluence measured with the EPID is back-projected to a plane above the patient dataset and then used as input for a 3D dose calculation in the planning CT dataset of a patient. The resulting reconstructed 3D dose distribution is then compared with the planned 3D dose distribution for that patient, providing information about possible differences between the two calculated dose distributions.

Two approaches of transit dosimetry back-projection dose reconstruction (Figure 2d) can be distinguished. In the first approach, the photon fluence measured with the EPID is back-projected through the phantom or patient to a plane above the patient dataset and then used to calculate the 3D dose distribution in the phantom or patient geometry. In the second approach, the dose distribution measured with the EPID is directly back-projected in the phantom or patient CT dataset. These transit back-projection methods may provide point dose (zero dimensional [0D]), 2D, or 3D dose distributions in a phantom or patient.

3 PHYSICS, MODELING, AND ALGORITHMS

3.1 Pretreatment Verification Methods (Non-transit Dosimetry)

In this section, the basic principles of non-transit EPID dosimetry methods as implemented in commercial systems will be reviewed, while details of the algorithms are provided in Appendix A.

The most common approach to EPID based PTQA is 2D verification, like the PFF method using detector arrays. VMAT verification presents challenges, as the gantry-angle dependence of the dose cannot be obtained from the image alone without other information. Compositing of the dose from all angles for a VMAT arc onto a single image is not recommended as adequate VMAT assessment using the TG 218 recommendations (Miften, Olch et al. 2018). Commercial methods that utilize time-resolved cine images for VMAT dosimetry have been hampered to date by lack of or limited access to these images provided by the EPID vendors.

3.1.1 Non-transit Dosimetry Using the Forward Approach

3.1.1.1 Image Prediction and Comparison: There are two different major method classes for non-transit 2D EPID dosimetry. The first is to compare the measured image with a prediction of this image. The use of a separate dose calculation algorithm is an acknowledged limitation of this approach, which has only some features in common with the TPS calculation such as, for example, an incident fluence model. Advantages of the

approach are that the physics of EPID image formation, including the energy-dependent response, can in principle be comprehensively modeled. Examples of commercial systems that employ this methodology are the Portal Dosimetry (Varian Medical Systems, Palo Alto, CA) product (Van Esch, Depuydt et al. 2004) and the Adaptivo system (Standard Imaging, Middleton, WI) (Olch, O'Meara et al. 2019).

3.1.1.2 Dose in Virtual Water Phantom: The second major class of methods is to utilize a model to convert the measured image to a dose in a plane of a virtual water phantom. Advantages of this method are that it (potentially) allows comparison with the TPS calculation in water for the IMRT beam or VMAT arc, while disadvantages are the uncertainties introduced by the EPID to dose conversion model. This method is common in commercial systems and corresponds more closely with established PTQA practices using other dosimetric devices than the image prediction and comparison method.

Furthermore, there are two major subclasses of algorithms used to convert the EPID signal to dose. The first is a "calibration" methodology. These are based on look-up tables which convert EPID signal at a pixel location to a dose value. The look-up table conversion factor will generally be a function of the equivalent field size estimated at the pixel off-axis distance and may include the fraction of fluence due to primary and multileaf collimator (MLC) transmitted beam. The latter is used for corrections for the difference in EPID response to primary and MLC transmitted beam (Wang, Gardner et al. 2009). These look-up factors can be determined from empirical measurements as a function of field size and off-axis distance. Advantages of these methods include the simple methodology, while a disadvantage is that the short-range EPID scatter is not accounted for, as a kernel is not used. Examples of these types of algorithms include Epiqa (EPIdos, Ivanka pri Dunaji, Slovakia) (Nicolini, Fogliata et al. 2006) and the PerFRACTION system (Sun Nuclear. Melbourne, FL).

The second subclass includes kernel-based approaches. This generally involves the application of a deconvolution kernel to the EPID image to estimate incident fluence followed by a convolution of fluence with a water scatter kernel to estimate dose at a depth of interest (Warkentin, Steciw et al. 2003). A single convolution kernel can also be used to convert EPID signal directly to dose (Ansbacher 2006). Advantages of these methods include more comprehensive modeling of the EPID scatter than calibration methods. EPID scatter kernels have been derived from Monte Carlo modeling of dose deposition in the EPID phosphor layer and, in some cases, modeling of optical photon deposition in the photodiode layer (Blake, Vial et al. 2013). An example of these types of algorithms includes the EPIbeam system (DOSIsoft, Coral Gables, FL) and EPIDose (Sun Nuclear, Melbourne, FL).

Commercial solutions generally apply the above methods to integrated images of the entire IMRT fields or VMAT arcs or, in some cases, over relatively large subarcs. Noncommercial evaluation methods have been developed for VMAT that compare 2D doses over small sub arcs with cine images; however, registration of the measured and planned or predicted doses is challenging. Calculation of dose in the TPS has been performed posttreatment to align the subtended angles of the dose calculations to the subtended angles of the acquired images

(Adamson and Wu 2012). A more subtle approach is to include a time dependence in the γ calculation to account for the problem of registration (in time) of the calculated and measured doses (Podesta, Nijsten et al. 2014).

3.1.2 Non-transit Dosimetry Using the Back-Projection Approach—Dose from the EPID image can be reconstructed in a patient geometry, i.e., using the planning CT images. Methods include adaptation of transit dosimetry algorithms to calculate dose without the patient present. An early method derived incident fluence from the EPID image by kernel deconvolution. The incident fluence was then input to a dose calculation engine as implemented in RadCalc EPID (RCE) (LAP, Boynton Beach, FL) (Renner, Norton et al. 2005). The kernel is derived in a fitting procedure to match doses measured in water.

3.2 Transit Dosimetry Methods

EPID-based transit images or 2D dose measurements can be compared with predicted dose data at the EPID level using a forward approach, while a comparison of the reconstructed dose with the predicted dose in the patient dataset requires a back-projection approach. In this section, the basic principles of these two approaches as implemented in commercial systems will be reviewed, while details of the algorithms are provided in Appendix B. Some applications of transit dosimetry in ART and future developments concerning real-time transit dosimetry will also be discussed in this section.

3.2.1 Transit Dosimetry Using the Forward-Projection Approach—During EPID-based verification using the forward transit approach, a measured EPID image is compared either with a predicted image or a predicted 2D dose distribution. In this method, which is based on image or dose values calculated using an independent image or dose calculation algorithm, errors in the data transfer and delivery of the treatment can be determined, as well as patient-related errors such as anatomy changes. A relative comparison of an EPID image made during a specific fraction with a reference image can also be made. Such a procedure will only identify variations in the treatment delivery over a series of treatments and may therefore miss some types of systematic planning and delivery errors. However, performing trend analyses, i.e., looking for changes over various treatment fractions, is a useful approach to help in deciding possible actions in the clinic as discussed in section 4.2. It should be noted that deviations in transit 2D EPID image/dose, observed by both forward approaches, are not related to variations in the actual 3D dose distribution inside an irradiated patient in a simple way because the dose is calculated at the level of the EPID. Even if the dose is calculated as dose to water, this correlation is not straightforward.

The PerFRACTION transit dosimetry system has several options: relative 2D transit delivery monitoring, absolute 2D dose verification, and a 3D dose distribution reconstructed in the patient dataset (planning CT or Cone-Beam Computed Tomography (CBCT)) using delivery information from the machine log files and/or detected MLC positions from the EPID.

The Adaptivo software can measure a 2D transit image with an EPID, which can be compared with a predicted EPID image (gray level values) calculated by an independent image prediction algorithm. Automated integration is only available for a Varian linac with ARIA/Eclipse system. The software provides γ analysis with customizable percent

dose-difference and distance-to-agreement tolerances, 2D visual analysis of distributions, and comparison of dose profiles.

The SOFTDISO (Best NOMOS, Pittsburgh, PA) software applies γ analysis between two EPID portal images, using global 3%/3 mm criteria with the percentage of points with γ value smaller than one and the mean γ value as metrics. It allows visualization of an EPID image of one fraction to an earlier fraction, their γ analysis, and the resulting in-plane EPID dose profiles of two measurements acquired on two different days (see Figure 3).

3.2.2 Transit Dosimetry Using the Back-Projection Approach—In the back-projection approach, dose distributions are reconstructed within a patient anatomical model. If the anatomical model is a realistic representation of the anatomy during treatment (e.g., verified by means of CBCT), then this is an estimate of the actual delivered dose. If the anatomical model is the planning CT, then this method provides an estimate of the change in dose compared with the planned dose in the patient. It should be noted that this estimate is made based on the total fluence attenuation change at the proximal and distal side. Depending on the system, the comparison between the EPID-based dose distribution and the planned patient dose distribution can be performed in 0D (averaged over a very small volume), 2D, or 3D. The main advantage of back-projection compared with forward systems is that observed deviations have a more direct clinical interpretation if the anatomical model is the planning CT or CBCT.

The EPIgray (DOSIsoft, Coral Gables, FL) point dose (0D) transit dosimetry system uses the transmitted signal on the EPID to reconstruct the dose at points of interest within the patient. The dose reconstruction method uses a back-projection of the transit EPID dose onto the patient planning CT, as discussed in more detail in Appendix A. The reference dose values are obtained from the TPS. Any dose deviation is expressed relative to the values given by the RT Dose file in the TPS. Measured vs. calculated dose comparison can be performed in multiple user-defined points in the patient volume but not over the whole EPID area. If sufficient points are chosen, they are defined to represent target volumes and OARs, after which EPIgray produces statistics and DVHs. Analysis is performed in terms of relative and absolute dose deviations, also with γ-index evaluation. The software is available for Varian, Elekta, and Siemens linacs, their associated EPID panel models, both MOSAIQ and ARIA oncology information systems, and all major TPSs. Dose comparison and γ analysis are automatic, yielding a 3D display in situ, and there is an automatic notification system of alerts.

The 0D transit dosimetry portion of the SOFTDISO software involves a daily dose reconstruction at isocenter and compares this daily measured dose with the dose at isocenter from the treatment plan (see Figure 3). 3D dose calculation is performed. Additionally, 2D images are collected during all fractions and compared with the fraction #1 image, as discussed in section 3.2.1. The transit dosimetry analysis can be performed on 3D conformal, IMRT, and VMAT treatment plans, and the software is compatible with linacs from Varian, Elekta, and Siemens.

EPID-based 3D dose verification based on transit measurements has been implemented in two commercial systems, each applying a different technique for dose reconstruction. In the RCE software, the photon fluence measured with the EPID is back projected through the patient to the target of the linac and then used to calculate the 3D dose distribution in the patient geometry using a forward dose calculation. The RCE transit dose software allows the user to verify the delivered dose to the CT dataset of a patient or phantom during treatment through transit measurements with a patient or phantom in the beam path. The calculated 3D dose distribution can be displayed on a CT dataset, i.e., planning CT, phantom geometry, or even CBCT if appropriate consideration is given for the variation in HU relative to the planning CT. The software that is used for pretreatment 3D dose verification is discussed in section 3.1 and in more detail in Appendix A.

A previously commercially available system iViewDose (Elekta, Stockholm, Sweden, no longer available for sale) was originally developed as an in-house system at the Netherlands Cancer Institute (Wendling, McDermott et al. 2009, Mans, Remeijer et al. 2010). It is described here because of its contributions to the scientific methodology and the clinical experience gained with it. This system used a different approach in which the 2D dose distribution measured with the EPID was back projected in multiple planes in the 3D patient planning CT data. The dose calculation algorithm used in this system was a pencil-beam type, like that currently in RCE, because it was fast and relatively easy to implement. Beam modeling could be performed using either a generic model to be applied for identical linacs and beam energies or a more time consuming but slightly more accurate full commissioning process. The model parameters were based on commissioning performed with solid water and did not account for tissue inhomogeneities accurately. For treatment sites with inhomogeneities present, the in aqua vivo approach could be used (Wendling, McDermott et al. 2012). In aqua means that, before dose reconstruction, the measured EPID images were first converted to a situation as if the patient consisted entirely of water, and then the dose comparison was made with a planned dose distribution that was also calculated in the “water-filled patient.” For IMRT verification, the iViewDose acquisition software integrated the total signal of all EPID frames between beam-on and beam-off into one accumulated portal image. For VMAT verification, cine-mode image acquisition was used, and separate EPID frames were continuously acquired during delivery, while each recorded frame was associated with a gantry angle (Mans, Remeijer et al. 2010). The EPID spatial location was assessed by matching the portal image contour to the beam outline of the field (read from the TPS).

3.2.3 ART Applications—The actual dose delivered to a patient may deviate considerably from the planned dose due to variation in anatomy during radiotherapy. Underdosage of the target volume or overdosage of an OAR may require an ART approach, i.e., an adaptation of the treatment plan based on imaging performed during a patient’s treatment course to account for anatomical changes. These changes occur frequently, for instance, during the treatment of cancer in the thoracic and head-and-neck (H&N) region, which may require an adapted treatment plan based on onboard imaging during daily patient setup. Inspection of CBCT scans is the most frequently used process to decide if replanning is required.

The dosimetric impact of anatomical changes on various structures may vary depending on the treatment site and the position of the target volume and OARs. However, OARs are often located in or near regions with a large dose gradient, thus requiring accurate knowledge of the position of an OAR with respect to the beam geometry. Verification of the OAR position is therefore a prerequisite for assessing the actual dose in an OAR.

Transit dosimetry using EPIDs in principle can detect the effect on the dose delivery of anatomical changes during fractionated radiotherapy, either to the patient using the back-projection approach or at the position of the EPID using the forward approach, as discussed in section 3.2.1. Some systems (e.g., PerFRACTION and SOFTDISO) compare the transit EPID dose/image of the first fraction against that of other fractions in a treatment course relatively and therefore can detect interfraction treatment variations due to anatomical changes that may require replanning (Olch, O'Meara et al. 2019).

The use of CBCT images for 3D dose calculation to assist in identification of plans needing adaptation is challenging. The main reasons are image artifacts, limited field of view, and lack of proper HU calibration (Fotina, Hopfgartner et al. 2012). However, the lack of proper HU calibration was addressed by many investigators (Schroder, Stankovic et al. 2020). The use of deformable image registration (DIR) would be an option, depending on the field of view and image quality. DIR would provide valuable information about the position of the clinical target volume and OARs. However, the use of DIR will introduce additional dose uncertainties, necessitating manual adjustments of contours. While significant attention has been given to DIR validation, establishing more rigorous validation methods remains a problem. Furthermore, there is currently a lack of automation and integration of DIR applications in an overall workflow. CBCT is currently likely the best method of detecting anatomical changes during treatment that can be incorporated in an ART approach. Time-resolved EPID dosimetry may also improve the detection of these changes (Persoon, Podesta et al. 2016). In addition, more studies are needed on how to apply verification of adaptation during VMAT delivery. Integrated images are not very sensitive to these changes, whereas cine images over certain sub angles are likely to be more sensitive.

ART is resource intensive because it requires a replanning process, necessitating additional use of planning equipment and staff time. Furthermore, any adaptation of a plan also requires an additional PSQA verification, either with a phantom measurement before the next fraction is delivered or *in vivo* during that fraction, thus further increasing the workload. To limit the workload, tools should be developed to select patients who are expected to benefit from plan adaptation during a treatment course. Transit dosimetry might play a role in this selection process.

3.3 Limitations, Applications, and Challenges in Clinical Implementation of EPIDs

While there are many useful properties of EPIDs for PTQA and transit dosimetry, there are also many challenges. The most obvious drawback from a dosimetry perspective is the energy-dependent response of the EPID due to the structure of the EPID itself with the high atomic number of the copper buildup and gadolinium oxysulfide scintillation layers. These result in a response that increases with decreasing incident x-ray energy due to photoelectric absorption (McCurdy, Luchka et al. 2001). While these materials improve sensitivity for

imaging, they introduce many complex issues for dosimetry. For measurements made in air, there are several major dosimetric effects.

The EPID exhibits a strong response change to the primary beam with off-axis distance for flattened beams due to the variation in incident primary-beam energy with off-axis distance. This can be seen in a raw (nonflood field corrected) EPID image which has severe horns off axis. This is usually not seen by the user for clinical in-air images, as it is compensated by the flood-field image, which also contains these horns.

Another primary-beam effect is the difference in response to open and MLC transmitted beams, as these have very different energy spectra. The magnitude of this response difference has been modeled and measured as approximately a 30% response change (Li, Siebers et al. 2006, Greer, Vial et al. 2007). As most systems calibrate the EPID using an open beam spectrum, this tends to result in errors in EPID dosimetry for regions where a large component of the signal is due to MLC transmission. Some commercial systems have corrections built in for this effect by estimating the contribution of each pixel's signal due to open and MLC transmitted beams.

This energy-dependence will also affect the response to scattered radiation from the linac head and the MLC. As this scatter varies with field size, this energy dependence may also affect the field size response of the EPID (Parent, Seco et al. 2006). A large overresponse to changes in field size is evident with EPID for higher incident beam energies, as the head scatter at these energies is not absorbed by the relatively thin EPID buildup layer (Gustafsson, Vial et al. 2009). Generally, IMRT and VMAT are performed at lower 6–10 MV energies, where this effect is not as evident. Most commercial systems include a field size response correction, either through measurement and look-up tables, or kernel fitting.

For transit dosimetry measurements, similar issues arise; however, there is the effect of the patient on the energy fluence incident on the EPID. The energy of the primary beam will be modified by the patient attenuation, and this will in turn depend on off-axis distance for flattened beams (Nijsten, Van Elmpt et al. 2007). The energy of scatter from the patient to the EPID can also depend on patient thickness and field size, as well as distance from the patient to the EPID. While challenging, these factors can be accounted for either using sophisticated models of EPID response or with empirical or model-based corrections to the EPID images.

Some research is being undertaken to modify the construction materials (i.e., to remove the high atomic number phosphor layer) to measure direct energy deposition in the amorphous silicon layer or to replace the phosphor with plastic scintillators (El-Mohri, Antonuk et al. 1999, Moran, Roberts et al. 2005, Blake, McNamara et al. 2013). These methods have been shown to produce measurements that are close to water equivalent. However, these types of EPID systems are not commercially available to date, as they generally result in a degradation of image quality.

The flood-field correction is important to remove nonuniformities in pixel response that would affect both imaging and dosimetry. All measured images are divided by the flood-field images, which also removes any information on the incident primary beam fluence

profile including any asymmetries (because these are in both the numerator/image and denominator/flood-field image). Therefore, measuring off-axis fluence properties of the beam is very difficult, and this can result in errors in the EPID derived dose. Some systems allow the application of a profile correction matrix to "restore" the beam profile using a d_{max} in water profile. However, if the beam profile in water varies, then these would have to be updated to reflect the true dose profile. Alternative calibration methodologies have been developed that use a pixel sensitivity map (PSM) that separates pixel nonuniformity and EPID off-axis response (Greer 2005, Parent, Fielding et al. 2007, Cai, Goddu et al. 2018). A regression-based approach to compute the pixels sensitivity map of linear accelerator portal imaging devices have been developed (Ahmad, Nourzadeh et al. 2021). The EPID image then contains the inherent EPID off-axis response to the incident fluence; however, this is not equivalent to a dose in water profile due to the strong energy dependence of the EPID.

Another feature of the flood-field calibration is the effect of the severe horns in the flood-field image and (raw) measured image profiles when the EPID is not positioned at the same position used for flood-field calibration. This will produce an artifact due to the incorrect division of the raw and flood-field off-axis horns (Greer 2005). The EPID position cannot thus be adjusted even though this would enable larger asymmetric fields to be measured. PSM methods allow the EPID to be positioned anywhere without introducing artifacts. A form of PSM approach has been implemented in the Adaptivo system to allow for EPID movement.

Additional limitations of EPID dosimetry for PTQA have been the saturation of signal for high dose-rate FFF beams with existing EPID systems. New generation systems have been released by both major vendors that support FFF beam imaging. In these cases, the majority of PTQA EPID methods can be adapted to FFF. For Varian aS1000 panels, FFF beams can be used for TrueBeam systems with software version 2.0 or higher and with the source-imager distance (SID) increased to 125 cm for 6XFFF and 165 cm for 10XFFF beams.

Consistency and linearity of the EPID response to delivered dose is important. Drifts in the EPID response can occur over time due to radiation damage. These can be off-axis dependent and require monitoring and correction. Most studies have demonstrated that modern a-Si EPID designs are very robust and stable (Barbeiro, Parent et al. 2019). Nonlinear response effects including image lag and ghosting have been observed and corrected, mainly for low MU (McDermott, Nijsten et al. 2006, Cai, Goddu et al. 2018). More recently, some of these effects have been attributed to incomplete frame collection. When all frames including those with partial signal at the start and end of irradiations are included in the image, then nonlinear effects were found to be negligibly small (Podesta, Nijsten et al. 2012). Long term reproducibility of the Varian system has been demonstrated to be <1% (all pixels) over a three-year period (King, Clews et al. 2011) and of the Elekta system was demonstrated to be <0.5% (all pixels) over nearly two years (Louwe, McDermott et al. 2004).

The size and the position of the EPID detector can be a limitation for treatment verification, particularly for large and asymmetric fields. The Elekta EPID is positioned at 160 cm from

the source, and therefore, PTQA is limited to fields with extents less than 12.5 cm from the central axis. While it is possible to position the Varian EPID closer to the source for PTQA and to measure larger fields, the aS1000 system is still limited to field extents 15 cm from the central axis in the cranial-caudal direction. For transit dosimetry, the Varian EPID must also be positioned at sufficient distance to clear the treatment couch, which limits the field size.

Alignment of the EPID image/dose matrix with the reference image/dose is required before analysis. There are two main approaches that are employed. The first is based on a central axis pixel location which may be predefined (fixed) or may be determined and updated in a calibration procedure. The second is to register the EPID matrix and the reference matrix either manually or automatically to account for any displacement. However, this has the disadvantage that it could potentially mask systematic positioning errors in the delivery of the dose. Another consideration is that the EPID position can vary with gantry angle due to sag of the support arm structures, and this can be several mm in some cases. The Varian IsoCal system can be used to determine the offsets of the imager panel from isocenter with gantry angle. On C-Series linacs, a software correction is applied to measured images, whereas on Truebeam platforms, active panel position corrections are made. If integrated images are acquired for VMAT delivery, without active or software correction of individual frames, then the influence of EPID sag will be present in the summed integrated image.

An issue that is only present for Varian EPIDs is the effect of backscatter from the metallic support arm for the panel, which has components directly underneath the active detector layer. This backscatter gives an additive component to the EPID signal that depends on the fluence from the field impinging on the support arm (Ko, Kim et al. 2004, Rowshanfarzad, McCurdy et al. 2010). The actual backscatter contamination to the measured image is even more complex, however, as the flood-field correction image has itself a large additive backscatter component. The backscatter in the measured flood-field corrected image is therefore the backscatter component in the raw image of the field divided by the backscatter component of the flood field, which makes it field size dependent and nontrivial to correct. A simple method has been proposed that corrects the backscatter component present in the flood-field correction image (Greer, Cadman et al. 2009). This improves results for smaller fields, and a similar approach has been implemented in the Portal Dosimetry preconfiguration package (Vinall, Williams et al. 2010, Van Esch, Huyskens et al. 2013). Other systems have implemented more advanced field size–dependent correction methods using kernel-based predictions of backscatter (Rowshanfarzad, McCurdy et al. 2010, King and Greer 2013) or methods that correct images to produce symmetric profiles (Berry et al. 2010). The newer aS1200 Varian EPID has additional backscatter shielding layers underneath the active layer to absorb the backscatter, and these have been shown to be effective (Miri, Keller et al. 2016).

Some investigations have focused on improving the commissioning of the clinical EPID system. The Portal Dosimetry beam profile matrix that is applied to the measured EPID image was modified to improve agreement of predicted and measured images (Bailey, Kumaraswamy et al. 2009). The manufacturer has also released a standardized deployment

package designed to be used without local parameter optimization to reduce workload and improve standardization.

A limitation of the EPID for VMAT dosimetry is that it rotates with the gantry, and use of an integrated image for each arc gives information like PFF or PC analysis. 3D dose or time/gantry-resolved information for VMAT therefore requires the acquisition of image frames (or cine images) with gantry rotation and a means to assess the gantry angle-dependent dose delivery. This can be reconstruction of a dose within a phantom or patient dataset using the gantry angles of the acquired images (Ansbacher 2006, Miri, Lehmann et al. 2017, Alhazmi, Gianoli et al. 2018) or a form of 2D assessment such as subarc analysis (Liu, Adamson et al. 2013) or time-resolved γ analysis (Podesta, Nijsten et al. 2014). However, the provision of these cine images from vendors has been limited to date, and most commercial dosimetry solutions simply use the integrated image of the delivered arc with no gantry angle-dependent assessment. Individual frames have become available with purchase of license from Elekta for their EPID software (version 3.4.1 onward); however, these are not easily accessible from Varian on their aS1200 EPID system at present.

A subclass of time-resolved assessment is real-time assessment. Transit EPID dosimetry is currently only used commercially in an offline mode, i.e., the integrated dose is reconstructed and analyzed after the acquisition of EPID images is finished. Offline dosimetry is performed without the intent of interrupting the linac, and deviations from the intended dose delivery are generally known in a short time interval after the end of a fraction. Real-time transit dosimetry could catch severe errors during the patient irradiation, i.e., transit dosimetry used in an online mode with the intent of halting the linac in case of irreparable harm to the patient (Fuangrod, Woodruff et al. 2013, Woodruff, Fuangrod et al. 2015, Spreeuw, Rozendaal et al. 2016, Passarge, Fix et al. 2017, Bedford and Hanson 2019). This might be particularly important for hypofractionated stereotactic body radiation therapy (SBRT) treatments in which detected errors cannot always be compensated for in subsequent fractions. CBCT can detect certain types of patient anatomy changes, but real-time IVD can in addition catch machine delivery errors, inadequate immobilization, and human errors, e.g., accidental plan modification, incorrect treatment site or plan, which are unique to each fraction.

For transit dosimetry, the integrated image does contain useful information on anatomical change with all fluence changes from all angles combined. Integrated image signal changes during treatment with the fraction one image used as the baseline has been shown to be sensitive to patient positioning errors, tumor shrinkage, as well as volumetric change in H&N treatments (Lim, Tsai et al. 2019). Methods that combine gantry-resolved image prediction and integrated image acquisition have also been developed (Bedford, Hanson et al. 2014).

4 CLINICAL EXPERIENCE

4.1 Pretreatment Verification Techniques

4.1.1 Sensitivity and Specificity—EPIDs have become widely used to detect errors in planning or delivery as well as plan transfer due to the convenience of setup and

efficiency. In this capacity, errors in planning or delivery as well as plan transfer can be verified. EPID-based PSQA systems should be able to detect deviations between planning and delivery in cases when they are clinically relevant. Knowledge of the sensitivity and specificity of EPIDs in detecting errors is therefore a prerequisite to define alert criteria for their clinical use. For this purpose, the sensitivity and specificity of each EPID-based PSQA system to detect errors, the magnitude of these errors, and types of errors should in principle be assessed for relevant combinations of alert indicators, delivery techniques, and treatment disease sites. In this section, the results of some of the relevant studies will be briefly reviewed (Table 3).

Systematic testing of the sensitivity of these systems to introduced errors of varying magnitudes typically involves introduction of global dose errors, MLC positioning errors, collimator errors, and gantry errors (Bailey, Kumaraswamy et al. 2012, Fredh, Scherman et al. 2013, Bresciani, Poli et al. 2018, Wu, Hosier et al. 2012). The Portal Dosimetry system was found to be insensitive to a TPS dose commissioning error as this error was not included in the Portal Dosimetry algorithm.

EPID systems have been compared to other detector systems such as Delta4, OCTAVIUS, COMPASS, ArcCheck, 729 PTW (Fredh, Scherman et al. 2013, Vieillevigne, Molinier et al. 2015) and demonstrated similar or better results.

Sensitivity studies of the pretreatment relative dose image comparison option of the SOFTDISO and Adaptivo systems have not been published, but some preliminary clinical results have been reported for the SOFTDISO system, as will be discussed in the next section.

4.1.2 Clinical Results—Table 4 summarizes clinical studies for pretreatment EPID based PSQA. Results using clinical plans have been analyzed to determine performance and tolerance levels for various systems for IMRT and VMAT including FFF beams (Howell, Smith et al. 2008, Bailey, Kumaraswamy et al. 2012, Fogliata, Clivio et al. 2011, Nicolini, Clivio et al. 2013, Iori, Cagni et al. 2010, Koo, Darko and Osei et al. 2021). These reports can guide other users as to the likely performance of their system. However, ultimately, performance will depend on many factors, including the inherent accuracy of planning and delivery of the user as well as the user's commissioning of the EPID dosimetry system.

Several institutions have reported on experience of detecting errors with their in-house models during clinical pretreatment verification of IMRT (McDermott, Wendling et al. 2006, Van Zijtveld, Dirkx et al. 2006). A variety of error types were detectable including incorrect modelling in TPS and delivery of wrong patient plan.

Much less studied to date is the application of EPIDs for dosimetry of small-field stereotactic radiosurgery (SRS) deliveries (Ballangrud, Kuo et al. 2018, Covington, Snyder et al. 2019).

4.2 Transit Dosimetry Techniques

4.2.1 Sensitivity and Specificity—Sensitivity and specificity can be determined for EPID-based transit dosimetry systems by irradiating a phantom with plans having deliberately introduced errors (Vieillevigne, Molinier et al. 2015, Bedford, Hanson et al. 2018, Mijnheer, Jomehzadeh et al. 2018).

Detection thresholds for the RCE system have been determined from 20 VMAT patients for four clinical sites using the TG119 confidence limit formalism (Esposito, Bruschi et al. 2018). Errors were then introduced into four VMAT plans to evaluate the detection sensitivity.

Esposito et al. validated an evaluation method for assessment of the accuracy of a novel 3D EPID back-projection method in an anthropomorphic phantom using RCE IVD software (Esposito, Marrazzo et al. 2021). The results showed that the RCE algorithm was able to reconstruct dose distributions in all anatomical sites.

Another work by Esposito et al. used the REC EPID for 3D IVD for abdominal and pelvic SBRT treatments. This study demonstrated the effectiveness of EPID IVD in detecting errors for abdominal and pelvic SBRT (Esposito, Ghirelli et al. 2021).

The effectiveness of iViewDose in detecting deliberately introduced errors during VMAT delivery was also investigated by another group (Mijnheer, Jomehzadeh et al. 2018). In that study, an Alderson phantom was irradiated using four VMAT treatment plans (one prostate, two H&N, and one lung case) in which delivery, thickness, and setup errors were introduced. Out of a total of 42 serious errors, the number of errors detected was 33 (79%), and 27 out of 30 (90%) if setup errors are not included. The system was able to pick up errors of 5 mm movement of a leaf bank, a wrong collimator rotation angle and a wrong photon beam energy. A change in phantom thickness of 1 cm was detected for all cases, while only for the head-and-neck plans a 2 cm horizontal and vertical shift of the phantom were alerted. A single leaf error of 5 mm could be detected for the lung plan only.

Yedekci et al. investigated the error detectability of iViewDose for 10 prostate VMAT SBRT cases by introducing various types of errors (Yedekci, Biltekin et al. 2019). Their study showed that patient setup errors may escape detection; however, errors in linac calibration, MLC position, and patient anatomy were detected with transit dosimetry analysis. The results were like those of Mijnheer et al. (Mijnheer, Jomehzadeh et al. 2018), indicating that iViewDose could detect several serious errors in dose delivery, leaf bank position, and patient thickness during VMAT delivery, but errors in single leaf position, as well as in patient setup, could only be detected in specific cases.

A sensitivity study of the 2D option of the PerFRACTION software was performed by comparing integrated EPID images of each field of each fraction to those from baseline fraction images. Open field measurements without a phantom or couch intersecting the beam demonstrated that this system was able to detect position errors of the jaws, MLC, and couch with an accuracy better than 0.4 mm and 0.5° for collimator rotation error. Delivery with a 10 cm thick rectangular solid water phantom in the beam was able to detect a 0.2%

machine output error. The system identified about the same failing pixel regions for induced MLC shift errors in IMRT fields compared with MapCHECK2 measurements and Eclipse calculations. Using an anthropomorphic head phantom, setup errors as small as 1 mm and 0.5° were detected. The authors concluded that this system, using integrated EPID images, is in principle sensitive enough to identify positional, angular, and dosimetric errors during transit dosimetry measurements (Zhuang and Olch 2018).

The relatively small number of clinical cases, treatment techniques, and error types is, however, a limitation of these types of labor-intensive sensitivity studies using phantom measurements in which errors are introduced. In another approach, the sensitivity and specificity of the system are assessed by employing a receiver operating characteristic (ROC) analysis of EPID data in combination with patient-related variations such as patient shifts or expansion and contraction of patient's body contours. The sensitivity to treatment parameter variations of the iViewDose system was studied by Bojechko and Ford (Bojechko and Ford 2015). EPID measurements of nine IMRT plans of a no-error situation as a baseline were analyzed in 2D in the isocenter plane in combination with "calculated error plans" created in a TPS. The sensitivity of iViewDose to patient-related variations was further investigated in a study of Olaciregui et al. (Olaciregui-Ruiz, Rozendaal et al. 2019). In that study, patient errors were introduced by transforming the planning CT into an error CT dataset and further examined using ROC analysis using the area under the curve as metric. Both sensitivity studies indicated that iViewDose could detect several serious errors in dose delivery, leaf bank position, and patient thickness, but displacements in the patient's position and random variations in MLC leaf position were not readily detectable.

A general conclusion of all these studies is that sensitivity and specificity, and thus alert criteria, are site specific and depend on the combination of error type and alert indicator (metric). Tolerance and action limits for the various methods of pretreatment and transit PSQA are discussed in section 5, while recommendations are summarized in section 7.

4.2.2 Clinical Results—In the review paper of van Elmpt et al. (van Elmpt, McDermott et al. 2008), three types of errors were distinguished that can be detected by means of EPID dosimetry:

1. Machine-related errors: MLC leaf position/speed, leaf sequencing, collimator angle, beam flatness and symmetry, linac output, and gantry angle;
2. Plan-related errors: leaf attenuation, TPS model (geometry model, beam model, output factors, etc.), dose calculation, and delivery of a wrong patient plan; and
3. Patient-related errors: obstructions from couch support and immobilization devices, anatomical changes in a patient since planning CT, uncorrected patient positioning, underdose or overdose in a volume of interest, anatomical movements during treatment, and wrong patient.

Several machine- and plan-related errors can be detected both by pretreatment and transit dose verification. Patient-related errors are due to changes in the patient's setup or anatomy compared with the situation at planning and can therefore only be detected with transit dosimetry. Table 5 summarizes some of these types of errors discovered by various groups

through EPID-based transit dosimetry (Mijnheer 2017[b]). These examples are described in papers published after the review article on EPID dosimetry by van Elmpt et al. (van Elmpt, McDermott et al. 2008). These and other examples have been discussed further in an updated literature review by McCurdy et al. (McCurdy and McCowan 2017). Some of them are also discussed later in this section.

The first results of the clinical use of the PerFRACTION software, which automatically compares in a relative way new images against baseline images using γ analysis, has been reported (Olch, O'Meara et al. 2019). Integrated EPID images were collected for 855 fractions of 60 treatment courses for 57 patients. Two tolerance settings of 2%/2 mm and 3%/3 mm were used for analysis. Here, 18% and 8% of all fractions and 60% and 28% of all courses failed for the two tolerance settings, respectively. For 3%/3 mm tolerances, the fraction failure rate for the brain, extremity, and spine treatment sites was the lowest, whereas the abdomen, chest, and H&N failed more often.

Interestingly, IMRT had higher passing rates than 3D conformal radiation therapy (3DCRT). The PerFRACTION software was used clinically for a large group of patients to analyze transit dosimetry EPID images of 32,632 fractions of all patients receiving photon treatment in 2018–2019 in the Iridium Kankernetwerk, Belgium center (Bossuyt, Weytjens et al. 2020). In a subgroup of 24,011 fractions from 3671 patients, absolute verification was performed, allowing comparison of images with calculated predicted dose distributions. Parameters for γ analysis were empirically determined, balancing the rate between detection of clinically relevant problems and the number of false positive results (see Table 5). In this group, 3766 fractions failed (16%), of which 6% were false positives and 10% were caused by patient-related issues. Causes for failed analysis included deviations in patient positioning and anatomy change such as weight loss, deviations in bladder or rectal filling, and tumor shrinkage. In addition, errors in planning, imaging, treatment delivery, simulation, breath hold, and with immobilization devices were detected. The authors concluded that EPID-based pretreatment and transit dosimetry using this system efficiently revealed a wide variety of deviations and showed potential to serve as a basis for adaptive planning.

Clinical experience with EPIgray has been described for both Elekta (Ricketts, Navarro et al. 2016, Ricketts, Navarro et al. 2016) and Varian equipment (Celi, Costa et al. 2016). In the study by Ricketts et al. (Ricketts, Navarro et al. 2016), measured EPID dose maps of 58 patients were back projected using planning CT images to calculate dose at prespecified points within the patient and compared with TPS dose using point dose differences. In their study, 83.8% of all delivered beams achieved the initial set tolerance level of 0 ± 5% dose difference, while the protocol also detected that 3 out of 20 measured prostate patients had undergone anatomical changes in comparison with the planning CT. Celi et al. (Celi, Costa et al. 2016) described the results of a 2-year period of 34,107 verification measurements of 3163 patient plans using EPIgray. A comparison of the TPS doses with the doses estimated by EPIgray showed a mean difference of 1.9 ± 5.2%. Further analysis indicated that lateral breast treatments at their center generally result in better dosimetric conformance than supine breast treatments. Consequently, a manual realignment procedure of the images was performed for the breast/supine treatment verifications above tolerance.

Before this correction, 21% of breast/supine treatment verifications were above tolerance, which reduced to 5.7% when the correction was applied.

A prostate study discovered that beams and arcs with out-of-tolerance IVD results tend to have more complex modulation. Both publications revealed that EPIgray was able to identify several anatomical changes and patient setup inaccuracies that could lead to unacceptable dose delivery errors.

In a recent large clinical study, the experience with SOFTDISO for the verification of more than 800 patients has been reported (Piermattei, Greco et al. 2018). The results showed that application of SOFTDISO allowed the authors to detect on average 6% of VMAT plans and 21% of 3DCRT plans outside at least one of their tolerance levels. Both studies concluded that SOFTDISO was able to detect treatments where delivery was inconsistent with the original plan, allowing physics and medical staff to promptly act in case of major deviations between measured and planned doses. The tolerance levels applied in this study were (i) the R ratio between the reconstructed and planned isocenter dose of ≤5% and (ii) a γ pass rate ≥90% and $\gamma_{mean} \leq 0.4$, (iii) γ parameter = 3%/3mm for VMAT and 5%/10mm for 3DCRT respectively.

In a recent paper, 5 years transit EPID dosimetry data obtained using the 0D option of the RCE software were presented (Nailon, Welsh et al. 2019). The difference between transit dose measurements obtained by RCE and point doses calculated by the Eclipse TPS were analyzed for a large cohort of 3795 patients treated with VMAT and 3DCRT. A total of 153 plans exceeded the ±10% alert criterion, which included 7.9% of the breast treatments, 4.4% of the H&N treatments, and 3.5% of the prostate treatments. The study also showed that the 0D approach is straightforward and has been implemented as a therapist-led service with no disruption to the patient and no impact on treatment time. However, clinical experience with the 3D option of RCE has not yet been reported.

Clinical experience with the iViewDose software was reported in several publications. In a study by Hanson et al., IVD results of 1220 patients acquired over a period of 5 years were analyzed (Hanson, Hansen et al. 2014). The mean deviation between EPID based isocenter dose and expected isocenter dose for these patients was −0.7 ± 3.2%. As a result of these measurements, EPID-based IVD has replaced nearly all pretreatment dose verification of IMRT treatments in that center. Transit dosimetry results obtained in The Netherlands Cancer Institute in the period 2012 to 2014, for more than 15,000 patient plans, were analyzed per treatment site (Mijnheer, González et al. 2015).

Many alerts were observed, which were mainly attributable to limitations of the back-projection algorithm, anatomical changes of the patient between planning and treatment, setup errors, and deviations from the routine clinical treatment procedure. However, the mean difference per treatment site between measured and planned dose at the isocenter encompassing an area of 9×9 pixels over that period was small, generally within 1%, except for some treatment sites such as the breast. The γ evaluation results also indicated that, for most treatment sites, on average, no systematic difference existed between measured and predicted dose values.

5 CLINICAL IMPLEMENTATION

5.1 Commissioning, Calibration, and Validation

5.1.1 Commissioning and Calibration of an EPID System—The commissioning of an EPID system is well described in AAPM TG-58, published in 2001 (Herman, Balter et al. 2001). While the principles of commissioning an EPID system that is to be used primarily for portal imaging and patient alignment have not changed in a significant way since 2001, the technology incorporated into these panels has changed considerably. In TG-58, the two dominant technologies described are matrix IC-based panels and camera-based panels, while the dominant form of EPID technology used today are photo-diode arrays. That report also could not have envisioned the diverse set of applications that these panels could be used for, including both pretreatment IMRT/VMAT QA and transit dosimetry.

In addition to commissioning an EPID system for imaging and patient positioning purposes, several other aspects of the EPID should be confirmed to ensure that the EPID will function accurately as a dosimeter, including dose response, field size dependence, uniformity, and reproducibility (Greer and Popescu 2003, Louwe, McDermott et al. 2004, King, Clews et al. 2011). Table 6 lists the recommended tests along with a brief description and suggested tolerances. These tolerances are a suggested minimum performance level to utilize an EPID panel for dosimetric purposes and should match or be tighter than the vendor specifications. In situations where the vendor specifications are more relaxed than the recommended tolerances in the table, the user should exercise caution in applying the product/solution to treatments that require tight margins and/or a high dose per fraction. The tolerances on these tests may need to be stricter for certain treatment modalities, e.g., SRS or SBRT. These tests should be completed at a SID that is within the range of clinical use provided by the vendor and should match the SID that will be used for PTQA and transit dosimetry. Modern EPID panel models were designed with dosimetric applications in mind and should perform well in this setting. It is suggested that the users review the literature provided by the vendor as well as published research and review articles associated with their EPID panel before testing or implementation of any dosimetry solution to ensure that it is appropriate to use for dosimetric purposes. Validation of the EPID panel for either PTQA or transit dosimetry will be discussed separately in section 5.1.2.

5.1.1.1 Commissioning of an EPID System for Pre-Treatment QA: The commissioning of a pretreatment IMRT QA system is generally defined by the vendor, and the user typically does not have the ability to significantly modify the process. The commissioning of an EPID system for PTQA should be performed after the commissioning of both the linac and the EPID panel for general imaging use. While the different vendor solutions for PTQA have different requirements for the commissioning process, there are several similarities. The common workflow for commissioning these systems typically includes a two or three step process. First, a series of vendor designed measurements is made with the EPID panel. Then these measurements are imported into the vendor's software so that the radiation beam and the EPID can be modeled. Then some vendors have a separate calibration step for the EPID panel. Typically, many fields are delivered so that a range of linac and EPID characteristics

can be modeled, including field size effects, dose rate effects, scatter response, MLC transmission, and dosimetric leaf gap. Other aspects of performance that may be modeled consist of EPID ghosting, sag of the EPID panel at different gantry angles, backscatter radiation emanating from the support arm of the EPID system, etc. The images collected from these commissioning fields are then input into the vendor's software for modeling. The modeling process adjusts the system algorithm settings so that it incorporates the local user's radiation beam and EPID characteristics. It is worth noting that some vendors provide a solution that forgoes the commissioning of individual linac and EPID systems and instead utilizes a model generated from aggregated data from other linacs/EPIDs of the same variety. The time required for the commissioning of a PTQA system can vary significantly from vendor to vendor, from under an hour to many hours.

5.1.1.2 Commissioning of an EPID System for Transit Dosimetry: The commissioning process for a transit dosimetry system is like that of a PTQA system and generally follows the same steps. One significant difference is that the commissioning measurements are not exclusively in-air measurements but instead are performed through a scattering medium. The fields provided for the commissioning process perform a similar task to that described for PTQA commissioning, but typically, more fields are required to model different amounts of scattering media. The modeling of these data also generally takes longer than for PTQA due to the greater number of measurements and because of the increased complexity of transit dosimetry calculations.

Many vendor solutions for both pretreatment IMRT QA and transit dosimetry rely on calibration of the EPID panel. Generally, the calibration process consists of delivering a set amount of MU under reference conditions to the EPID panel so that the output of the EPID panel can be scaled appropriately to match the expected dose output of the system under these conditions, such that a dose value can be assigned to the EPID signal generated. Postprocessing of EPID images, including thresholding and smoothing, are not usually performed for the dosimetric purposes of these systems. Some systems perform auto-registration up to a few millimeters if enabled by the user.

5.1.2 Validation of Pre-Treatment QA and Transit Dosimetry Solutions

5.1.2.1 Pre-Treatment QA Validation: Before a PTQA system can be used clinically, the system must undergo a set of validation tests to ensure the system is working as intended. A set of validation tests that include a range of delivery patterns should be established to measure and verify the integrity of the system and generate a baseline, which can serve as a reference when the system requires maintenance. The delivery patterns should include fields that encompass all energies, field sizes, and dose rates on the linac with the specific imaging panel. These tests should include the ability to verify the portal imager is working correctly with the dosimetry system by consistently calculating the correct dose values with the correct geometrical dose distributions that fall within the expected clinical delivery parameters intended for the linac. It is recommended that fields and plans utilized during the validation of the TPS be reused during the pretreatment validation process to improve efficiency and consistency. Additionally, validation of each modality and energy to be utilized by the PTQA system should be completed, including step and shoot IMRT, sliding

window IMRT, VMAT, SBRT, SRS, etc. By completing the validation testing, the user should have established an understanding of the performance characteristics and limitations of the EPID and analysis system.

For the purposes of validation, it is expected that the TPS is already fully commissioned using equipment and methods with proven accuracy and that the set of treatment plans that were used for TPS commissioning is updated to the current TPS version and available to the user for the purpose of the EPID dosimetry validation. During the validation process, the user is expected to compare two datasets, namely, the TPS reference dataset and the EPID reconstructed dataset. In the case of 2D systems, 2D γ comparison of the 2D dataset provided by the EPID solution with the TPS would be performed. Where the EPID solution does not allow for comparison directly with TPS dose, export of dose and comparison in third-party software will be required. For systems that do not convert pixel values to dose (e.g., Portal Dosimetry, Adaptivo), the comparison of the EPID software predicted image (generated from the TPS reference data) with the EPID image is performed, as presented in Section 3. In the case of systems that produce 3D dose distributions in a phantom or patient geometry based on in-air EPID measurements (e.g., RCE), comparison can be made between the 3D dataset provided by the EPID solution and the TPS calculation using 3D γ analysis or multiple plane 2D γ analysis where this is not available. For 3D systems, the additional use of DVH comparison is also available. For γ analysis comparisons, the criteria recommended in TG 218 should be used.

Additional measurements to obtain dose to a point, a plane, or a volume can also be made. Such measurements would complement the existing TPS commissioning data and can be obtained at the discretion of the user. Most PTQA solutions will rely on 2D datasets from the TPS, PTQA prediction software, and 2D EPID images for comparisons and to complete the validation of the product. For some systems like PerFRACTION, the 2D dose is calculated at a specific depth in a virtual slab phantom from the acquired EPID image. The EPID is irradiated at a distance near the isocenter. To validate this 2D dose, one can transfer the TPS dose from the patient geometry to the identical slab phantom geometry just as one would do if the comparison was to a detector array. One could also use a detector array as the comparator instead of the TPS, but either is appropriate. A γ analysis (separate software may be required) should then be performed to determine the degree of agreement between the EPID system 2D dose and the reference dose (TPS or measured). Tolerances for these validation tests should be consistent with that used with a detector array per TG 218. Other established 2D plan QA methods can be helpful to build confidence of a new EPID based QA system—for example, statistical correlation between EPID and other QA systems can be verified (Wu, Hosier et al. 2012). It is also recommended that the induced error test described below be performed for PTQA as a final end-to-end test of the system used in the routine clinical mode.

Creating plans and fields with induced errors can be used to determine the sensitivity of a system in the detection of errors and to confirm that this detection sensitivity matches expectations and vendor specifications. Induced errors of known magnitude can be systematically applied to fields, and the γ failure rate of the EPID system can be compared with that of the error-free delivery relative to a trusted reference dataset. The

EPID distance that will be used clinically should be used for validation. A slab phantom that is representative of a human abdomen (for example 20 cm thick, 30 × 30 cm) should be utilized for these tests. Open and intensity modulated fields should be used to irradiate the EPID for validation of the system performance and its ability to detect errors. Basic field or arc-induced error tests created in the TPS (in the transit dosimetry geometry) should introduce known dose distribution changes and can include MLC positioning errors, incorrect positioning of the patient/phantom, or incorrect patient/phantom thickness. Note that the EPID system may be comparing the EPID dose rather than the TPS dose with a predicted dose. One *should* separately verify the predicted dose is accurate relative to a measurement (see Figure 4).

- The software utilized for predicting the EPID's response to radiation treatments should be used to calculate an induced error and error-free dose distribution at the SID (usually 100 cm) and in the plane and phantom consistent with the calculations of the EPID system. One should perform a γ analysis (either 2D or 3D) between the correct distribution and the perturbed one (using software separate from the EPID analysis software). Thus, one will have the known γ passing rate from the TPS-created fields as the ground truth (**Comparison 1**).
- The EPID should be irradiated, and the EPID dosimetry system should be used to evaluate the response from the correct fields as compared to the predicted EPID dose distribution from the correct fields (**Comparison 2**) to serve as a baseline against which the perturbed fields can be evaluated.
- Finally, the EPID is irradiated with the induced error fields and compared against the predicted EPID dose distribution from the correct fields (**Comparison 3**). The analysis should use the same dose, distance to agreement tolerances, and dose threshold as the other two comparisons.
- The passing rate of the EPID system for the correct fields will likely not be 100% (Comparison 2) due to changes in the EPID panel sensitivity relative to the day the system calibration images were taken, along with whatever image processing and pixel value to dose conversion errors take place in the EPID system. This passing rate should be at least 95% for dose difference, DTA, and dose threshold of 3%, 2 mm, and 10%, respectively.
- The γ passing rate from Comparison 1 should be compared with the passing rate of Comparison 3 corrected by the passing rate of Comparison 2, and that result should be within 5% (absolute) of Comparison 1. For example, if the passing rate of the TPS correct vs. induced error field is 90% (Comparison 1—this is the value we ideally want the EPID system to produce), the Comparison 2 passing rate is 98% (2% lower than a perfect measure of the error-free field), and the passing rate for the EPID analysis of the induced error field is 93%, then the corrected Comparison 3 passing rate is 93 + 2% or 95%. This value is within 5% of the Comparison 1 passing rate of 90%. If the EPID irradiations are all performed at the same time, then linac output and EPID panel sensitivity variations will not need to be considered.

- The ability for the EPID system to meet those tolerances may depend on the field size for the test fields used, with fields larger than 15 × 15 cm fields having larger errors than smaller ones.

5.1.2.2 Transit Dosimetry QA Validation: For back-projection systems such as EPIgray and SOFTDISO that calculate the dose in the patient dataset at representative points or the isocenter, 0D validation against the TPS system dose calculation at these points is required. This should be performed for individual open fields of various sizes and representative composite IMRT or VMAT dose distributions. To understand the system performance, both slab phantoms and anthropomorphic phantoms can be used. Sensitivity to errors should be examined, as described in the next section.

For transit dosimetry systems that provide 2D images for QA analysis, validation is performed at the SID of the EPID. For systems that calculate and compare with EPID image grayscale values directly, such as Adaptivo, comparisons of measured images with predicted images are performed. For systems that convert a transit EPID image to a 2D dose in a slab phantom at a specific depth (and acquisition SID) such as PerFRACTION, one should validate this dose by comparison with the internal dosimetry prediction algorithm of the EPID system. These systems generally calculate their own comparison dose from the treatment plan parameters. Validation testing should include an evaluation of the ability of the system to detect induced errors (see section 5.1.2.1 for suggested tests). Tolerances for validation of the image-to-image method should be the same as from TG 218, while tolerances for 2D dose comparisons may be more lenient based on the finding of the validation process and the clinical intent.

An independent dose comparison should be performed when feasible. The exact geometry of the EPID and slab phantom can be simulated in the TPS, or a detector array can be placed under the couch at the same source-detector distance (SDD) as the EPID for irradiation. These latter two methods of independent dose comparison may not yield excellent agreement with each other due to the difficulty for the TPS to accurately calculate the scatter dose contribution imposed by the phantom. Also, making an accurate measurement in this geometry with a detector array is challenging. Tolerances from the independent measurement method should be expected to be less stringent such that a 90% pass rate is achievable with 3% dose and 3 mm DTA, and that applies to the induced-error test in section 5.1.2.1.

For back-projection systems, the 3D dose distributions calculated in the phantom or patient dataset can be compared with the TPS calculation using 3D γ evaluations and/or DVH comparisons. Measurement of 3D dose distributions is not feasible for most clinics. The overall performance and sensitivity of the system should be evaluated for simple phantoms and phantoms that replicate clinical situations.

5.1.2.3 Validation of Advanced Treatment Techniques: Flattening filter-free (FFF) beams are available in many linacs, offering a high dose rate delivery mode. EPID dosimetry can still be implemented in high dose rate conditions, provided that the EPID signal does

not saturate during transit imaging. Newer systems from both major vendors are capable of imaging FFF beams under a wide range of conditions.

Whereas an EPID system has been shown to be well suited to verify machine isocenter prior to SRS delivery, the use of EPID dosimetry for patient specific pre-treatment SRS/SBRT QA presents some challenges. Although SRS plans were typically not part of the pre-treatment QA since they historically have been delivered via cones, static fields or dynamic conformal arcs, the use of IMRT and VMAT delivery and the recent adoption of single isocenter techniques to treat multiple brain metastases adds a complexity layer to SRS delivery and verification. Typical matrix array detectors do not have the resolution for small fields, so the higher resolution EPID is an excellent detector for this application. As mentioned above, FFF beams, often used for SRS, could saturate the EPID in older systems unless an SID greater than 150 cm is used. The EPID can also be used for periodic QA to ensure the geometric accuracy of the delivery (Chuter, Rixham et al. 2016, Pardo, Novais et al. 2016).

5.2 Routine QA for EPID-based QA systems

5.2.1 QA for EPID-Based PTQA Systems—To maintain optimal performance of an EPID-based QA system, a routine QA program must be put in place. Daily, monthly, and annual QA guidelines are discussed and given below, with focus on monthly QA, where a table is also included to help explain the topic.

5.2.1.1 Daily QA: For the QA of the EPID panel, the AAPM TG-58 recommends a daily check of imaging system functionality and collision interlock test. Although the tests recommended by this TG are mainly from an imaging point of view, failure of these tests could result in suboptimal function for dosimetric purposes. The most recent recommendations for MV imaging QA are included in AAPM TG 142 (Klein, Hanley et al. 2009), which includes checking EPID off-axis positioning/repositioning. The purpose of the positioning test is to ensure imaging and treatment coordinate coincidence. Positioning tests can be performed by imaging an object of known size with embedded fiducial markers, set to the isocenter, and using measuring tools at the treatment console, measure the displacement from imaging center to treatment isocenter. These tests should be performed at the cardinal angles to account for gantry/EPID sag. Some onboard imaging systems have the capability of accounting for the imaging arm sag by either mechanically repositioning the imaging detector or digitally shifting the acquired image. These calibrations should be completed before positioning tests are performed.

5.2.1.2 Monthly QA: The distance of the EPID panel from the source should also be checked, as it will affect dosimetric results and image scaling. This test can be performed by imaging a sheet with BBs on a 20 × 20 cm square at a clinical SID and measuring the scaling in the linac imaging software. Alternatively, per TG-58, one can physically measure the distance from the gantry (or laser) to the detector panel and compare it with the distance measured during commissioning. Physical measurements as such could be cumbersome, as they may require removal of the plastic panel guard. Some systems have EPIDs that do not retract and are mounted at a fixed SID. In these cases, physical imager distance can be measured during acceptance testing/commissioning followed by monthly geometric scaling

tests. The suggested tolerance for positioning and scaling is ≤2 mm for non-SRS/SBRT applications and ≤1 mm for SRS/SBRT-type applications. Accurate positioning of the EPID panel is essential to the accuracy of EPID-based QA systems (van Elmpt, McDermott et al. 2008), especially for complex plans with many gantry angles or continuous arcs.

The EPID dose response check should be performed after machine dosimetric output constancy is verified monthly. The EPID system should be calibrated based on a vendor recommended procedure, which typically involves delivering 100 MU with a 10 × 10 cm field size. Often, dark field is acquired to subtract the background noise, and flood field is delivered to divide out any response inhomogeneity of the panel. After the calibration, a large field should be acquired to be used monthly as a baseline for uniformity test (2D static field, Table 5). The field should be large enough to cover most of the panel but not to extend to the panel edges. The dose constancy of the EPID panel should be evaluated in absolute terms with a 10 × 10 cm field size. The dose measured with this test can be the reported central axis dose if it is provided by the user's software, or the user can manually acquire a mean dose of a small area around the central axis. The method chosen to measure the dose should be consistent for each QA. The dose constancy check should be performed monthly, and the panel recalibrated as necessary. A six-monthly recalibration is recommended and potentially more frequently for older EPID systems which may be less stable. The frequency of constancy checks should be increased for older equipment that require frequent calibrations. The trend of PSQA pass rates may also indicate drifting panel response and should prompt an additional constancy check (Table 7).

The system should be checked for constancy using plans or a subset of plans that were used for commissioning. These plans should range from simple static square fields to more complex ones such as VMAT. The VMAT measurements can serve as a pseudo–end-to-end test where output, gantry angles, dose rate, and MLCs are considered. These deliveries, along with beam profile tests, can be evaluated using γ analysis. If both IMRT and VMAT are used clinically, it is recommended to check both modalities. These measurements should be performed for all clinically used photon energies.

Dosimetry tests should be performed with the detector position as used clinically for pretreatment IMRT QA or as close to the gantry head as mechanically achievable. The smaller SID will allow the largest field size that can be measured on the detector without irradiating panel electronics. It is the responsibility of the clinical physicist to ensure that the machine output is within tolerances set forth by AAPM TG 142 (Klein, Hanley et al. 2009), ideally within 0.5%, before proceeding with dosimetry tests for EPID-based systems.

5.2.1.3 Annual QA: The second component of the EPID QA system is the third-party software. Once the software is commissioned and implemented clinically, the routine QA should follow recommendations of AAPM TG 53 (Fraass, Doppke et al. 1998) and the more current AAPM Medical Physics Practice Guideline 5.a. (Smilowitz, Das et al. 2016). These reports recommend that dose calculation tests should be conducted annually or after a software upgrade.

5.2.2 QA for EPID-Based Transit Dosimetry Systems—In principle, a transit dosimetry QA system is the same as a PTQA system but usually has more complex physics models that incorporate various factors into consideration such as the patient's scatter (section 3.2). As a result, transit dosimetry QA is generally considered less accurate than pretreatment when comparing with the TPS or predicted dose distribution (sections 3.2 and 5.1.2).

Consistency check of an EPID-based transit dosimetry QA system can be implemented in a very similar fashion to that for the PTQA system but with the addition of a physical phantom placed on the treatment couch for all measurements. This would ideally be a humanoid phantom, but solid water blocks or small water tanks are acceptable (section 5.1.2). The physical size and thickness of the phantom should approximate a typical patient setup. If possible, it is best to use the same phantom setup as the original commissioning setup. The baselines for transit dosimetry QA results should be acquired at the time of system commissioning (section 5.1.2). The detailed setup information, including phantom and EPID position, should be documented so that it can be reproduced in the future routine consistency checks. A similar or the same set of plans can be used for transit dosimetry consistency checks as for PTQA (section 5.2.2). Given the greater complexity involved with transit dosimetry, the tolerance levels can be relaxed compared with that of the consistency check of a PTQA system (Table 5). For example, when setting up solid water blocks or a small water tank on treatment couch (to simulate a patient) for such QA, the exact location of phantoms on couch, the type of couch top insert used, the relative positioning of EPID panel (particularly Elekta machines) to the phantom, can introduce additional errors in QA measurement, and thus result in possible larger variation in QA results. Although the Elekta iViewDose system is no longer available for sale, a new version of the software is commercially available as a tool for the Elekta Unity MR Linac (see Table 2).

It is important to be aware that the results of consistency checks of an EPID-based QA system could be potentially affected by many factors such as EPID panel performance and machine delivery. For consistency checks simple scaling factors due to machine output and EPID raw signal should be factored out; as an example, a 10×10 cm^2 field with standard MU can be acquired by the EPID at the same time of consistency check to "normalize" subsequent QA analysis.

5.3 Tolerance Levels for Patient-Specific QA

5.3.1 Introduction—Recommendations for error detection tolerances are provided in this section. These tolerances should be sensitive enough to detect clinically relevant errors while avoiding false positives for non-clinically relevant errors. Ultimately, each institution must decide whether their purpose is to discover gross errors only or if smaller but still clinically relevant errors should also be detected. One approach to determining tolerance levels is to begin with values in the table below but perform a statistical analysis on a sufficiently large number of institutional cases to find the best balance of false positive and false negative results (Bossuyt, Weytjens et al. 2020). This section is intended to apply to systems that either convert EPID pixel values (image signals) to dose or use the pixel values alone. For systems that convert to dose, this extra step involves additional uncertainty

that must be considered. Table 8 displays the achievable level of γ pass rates and dose differences for systems in clinical use for both pretreatment and transit dosimetry. A more detailed discussion of the clinical results of some of these studies can be found in section 4. On average, excellent agreement with the planned dose is generally achievable, but outliers exist. For transit dosimetry applications, these outliers are typically patients with setup or anatomic changes. These changes may be random such that evaluation of the mean passing rate of the fractions from the first half of the treatment course or on a rolling basis, for example, rather than any one fraction may be sensible.

Table 9 displays the tolerance levels for EPID-based systems chosen by various researchers as reported in the literature, like table III in TG 218. A more detailed discussion of the clinical results of some of these studies can be found in section 4. These values should be dependent on many factors, including patient-specific ones such as curative vs. palliative treatment intent, site, and the available resources to track down errors. Since the analyses have been performed after the treatment, the results do not necessarily apply to the next treatment. Presumably, a failed fraction will result in an examination of the treatment setup, delivery, and patient anatomy to mitigate the dose discrepancy for the next fraction. In section 4, sensitivity and specificity were discussed. In most instances, these will not be known very accurately for all sites and circumstances. Despite that, it is important to try to define them as well as possible. These factors, along with uncertainties in the dose accuracy of EPID-based systems, will combine to determine the detectability of the system. We would discourage the setting of tolerances solely based on the resources available to act on failures.

From the transit dosimetry data, it can be observed that some groups are using site-specific tolerance limits. This can be expected from the intrinsic property of transit dosimetry that its sensitivity for variation in setup and anatomy depends very much on the treatment site. Such a subdivision of tolerance limits needs, however, to be based on the clinical experience in a specific center and of course on the workload that is involved in the EPID-based IMRT and VMAT QA program.

Note that one group (Ricketts, Navarro et al. 2016) is using asymmetric tolerance limits for deviation of the dose at the isocenter for prostate vs. H&N transit dosimetry verification. According to these authors, this deviation is based on systematic differences for these sites between the dose calculation algorithm in the TPS and in the EPID dosimetry software, as well as anatomic changes and setup errors. Systematic differences between TPS and EPID measurements were also observed in another study (Nailon, Welsh et al. 2019), but that group chose a larger tolerance for the dose deviation at the isocenter of ±10% for all sites instead of using site-specific asymmetric tolerance limits.

For either pretreatment or transit 2D dosimetry analysis, it may be reasonable to use the mean pass rate for all the fields in the plan vs. failing the plan for any single failing field unless fields fail extensively.

5.3.2 Acceptance/Rejection Criteria for 2D and 3D PTQA and Transit Dosimetry

5.3.2.1 2D Pretreatment: The analysis methodology for a 2D EPID-based pretreatment γ analysis should be identical to that for any other 2D array. AAPM TG 218 should be used as a reference. The details of QA methods and data analysis can be found in sections 5.1.1.1 and 5.1.2.1. The PTQA section of Table 6 shows several publications which reported high passing rates when using the EPID, indicating that the passing criteria for PTQA should be like that achieved with detector arrays, typically greater than 95% of pixels passing 3%/2 mm with a 10–20% dose threshold.

5.3.2.2 2D Transit Dosimetry: For 2D transit γ analysis, there are currently two approaches to consider: (1) relative mode in which EPID images from each fraction are compared with a baseline image, usually the first fraction, or (2) absolute dose mode in which the EPID pixel values are converted to dose and compared with the "predicted" dose image based on the planning system data. In addition to the potential delivery errors, transit dosimetry involves the uncertainties in detecting patient-related errors in setup and anatomic variations, sometimes with organ motion involved. For relative mode, because no pixel-to-dose conversion takes place and the comparison is not related to the TPS dose, tolerances could reasonably be kept the same as for PTQA (Zhuang and Olch 2018). For absolute dose mode, tolerances should be relaxed compared with what is acceptable for PTQA due to additional uncertainties in the transport calculation through the patient and the treatment couch and the geometric scatter from the patient transmitted through 30–50 cm of air and couch. In contrast to pretreatment measurements, transit dose measurements include the variations in patient setup and anatomy from fraction to fraction. Relaxation of tolerances due to these changes tends to increase the specificity critical for clinical relevance and resource constraints but decrease sensitivity. A more appropriate reason to relax tolerances relative to PTQA is the specific patient treatment intent and other clinical considerations. For example, for a palliative treatment with little immobilization, small deviations in body pose, field position, or anatomy changes may not be important, and only gross errors of more than 5% would be relevant. Various reports in the literature have documented the dosimetric agreement for transit dose in clinical testing for IMRT and VMAT treatment, with anatomical changes being the dominant factor in determining dosimetric agreement. Nailon (Nailon, Welsh et al. 2019) reported absolute point dose agreement within 4% for a variety of treatment. Cilla (Cilla, Meluccio et al. 2016) reported that 93% of the studied H&N patients treated with VMAT passed a 3%/3 mm γ test. Piermattei (Piermattei, Greco et al. 2018) reported no γ failures for sites where tolerances of 3%/3 mm were applied; however, 17% of breast cases failed with tolerances of 5%/7 mm. These errors are caused by patient setup errors due to breast displacements of about 1 cm causing a deviation in the dose at the isocenter up to 7%, a gamma passing rate of 79%, and a mean gamma of 0.58. Once the patient setup was corrected, all these indexes returned within tolerance.

For 2D relative mode transit γ analysis, the passing criteria and tolerances are unrelated to the TPS dose and only reflect anatomic and setup variations from the baseline fraction vs. subsequent fractions as well as any changes in daily linac output (if not corrected for in the analysis software). For this constancy measure, based on the published high sensitivity of

at least one system to detect dosimetric errors in a 2D plane (Zhuang and Olch 2018), one could reasonably expect greater than 95% γ passing rate with 3%/2 mm in the absence of anatomic and setup errors.

For 2D absolute dose mode transit dosimetry, the criteria and tolerance may be relaxed due to the uncertainties of the dose conversion from the EPID image pixel data. The user should base the choice of acceptable γ passing rate both on what was achievable during commissioning and what others have reported in the literature. In any case, it appears that many systems can achieve at least a 90% γ passing rate with 5%/3 mm for a range of sites and treatment modalities.

5.3.2.3 3D Pretreatment: 3D pretreatment dose in the planning CT dataset can be calculated by acquiring an in-air EPID image for each beam and applying a deconvolution kernel to the measured distribution to remove the effects of the EPID on the radiation distribution, recreating the beam fluence as it exited the treatment head. This dose distribution can then be used to forward calculate the 3D dose in the planning CT. These steps impose uncertainty in the resulting 3D dose calculation which must be quantified at time of commissioning, so the choice of tolerances must include consideration for the system-specific uncertainty. The tolerance for 3D γ analysis for PTQA with EPID-based solutions should generally be the same as for the standard 2D and 3D detector arrays, following TG 218 guidelines.

5.3.2.4 3D Transit Dosimetry: With the 3D dose in the planning CT or CBCT, a 3D γ analysis structure by structure can be performed as well as DVH comparisons with the original plan. Some systems can calculate the 3D dose from only log files or a combination of log files and cine EPID images (log-based calculations are outside the scope of this report). As with EPID-based 2D transit dosimetry, reconstructed 3D dose should be compared with a well-established dosimetric method, such as the TPS dose in the planning CT using an inhomogeneous phantom with film or individual detector measurements (see section 5.1.2). If a system performs the back-projection on CBCTs, then a separate intercomparison should be made using the same phantom to evaluate the accuracy of handling the potentially smaller field of view, and artifacts in the CBCT.

The tolerance for 3D γ analysis for transit dosimetry will depend on the results of the intercomparisons mentioned above. It should be expected that the level of agreement that can be achieved with back-projection will be somewhat less than with 2D analysis. The studies by Mijnheer et al. (Mijnheer, González et al. 2015) demonstrated 85–93% passing rates for 3%/3 mm γ criteria for a variety of sites including SBRT, IMRT, and VMAT deliveries. It is impossible to correlate γ passing rate differences with the dose errors in patient anatomy. For this reason, comparing DVHs may be the most clinically meaningful analysis (Nelms, Opp et al. 2012).

5.3.3 DVH Analysis—One reasonable approach to DVH comparison is to use the same evaluation metrics for the EPID-based measurement as were used for the original plan approval but include an additional tolerance buffer to account for an acceptable degree of patient setup and anatomical changes. A good understanding of the limitations and

calculation methodologies of the user's EPID dosimetry system will enable a more informed decision about how much to adjust achievable in air tolerances to get clinically useful transit tolerances (Bresciani, Poli et al. 2018). During the plan approval DVH evaluation, patient- and plan-specific tolerances to deviations for both PTVs and OARs should be established for application to the DVHs from EPID-based daily QA. Wang et al. (Wang, Chen et al. 2017) found that DVHs for PTV and OARs were within 3% for D98% and mean, respectively. Where the OAR dose approaches known safe tolerance limits, for example, for spinal cord or brainstem, the radiation oncologist should carefully consider what to allow during daily QA.

Overall, selecting adequate but relatively simple metrics for DVH-based QA is still an evolving process. The various parameters that can be useful for comparison with the planned PTV dose are D98%, D95%, D90%, D2%; for OARs, mean, D1%, and maximum dose are often most relevant. Tolerances can be preset with dose analysis templates allowing for consistent data analysis and flagging of errors.

5.3.4 Evaluation of Failed Analyses

5.3.4.1 Pretreatment Dosimetry Failures: When PTQA fails, the same process for exploration of possible reasons for the failure as detailed in TG 218 can be followed except for checking phantom setup since EPID PTQA is performed in air.

5.3.4.2 Transit Dosimetry Failures: Failures should be evaluated to determine whether they really constitute a clinically relevant discrepancy that needs to be corrected. For 3D analysis, structure dose deviations are clearly understood, but this is not the case for 2D γ analysis, which is less intuitive. Approximations of correlation between the 2D error and 3D dose may be possible under certain circumstances, such as for AP/PA fields. If the magnitude of the error is clinically significant after accounting for any patient-specific considerations, then one should attempt to determine the reason(s) for the failure (Olch, O'Meara et al. 2019). Bossuyt (Bossuyt, Weytjens et al. 2020) provided a collection of examples of 2D failures for a wide range of circumstances.

The potential reasons are:

- Patient anatomy change
- Patient setup error
- External device in wrong place (entrance or exit)
- EPID panel positioning error, i.e., wrong SID
- Linac parameter does not match plan
- Linac delivery error

Methods for evaluation of the items above include the following:

- Review daily setup imaging, especially with CBCT, looking for anatomical changes that could explain failure.

- Review daily setup imaging and treatment history, looking for larger-than-normal shifts that could be indications of setup problems.
- Review daily setup imaging, looking for evidence of objects external to the patient that are not where they should be and are in the beam.
- Check treatment history, looking for mismatches of planned to delivered parameters.
- Check the treatment delivery device daily QA results, such as output and MLC positioning errors.

Please refer to Table 5 for a more complete list of possible reasons for transit dosimetry failures.

6 RISK-BASED ANALYSIS

As described in the AAPM TG100 report (Huq et al. 2016), physicists should use prospective risk assessment tools such as failure-mode and effects analysis (FMEA) and incident learning systems to guide the implementation of EPID-based quality assurance. While the differences in workflow between various EPID dosimetry systems precludes the use of a standard approach, examples of prospective risk assessment are also described in previous AAPM task group reports (such as TG 275 and TG 182), a work by Wexler (Wexler et al. 2017), and an online resource exists for guidance (see https://www.aapm.org/QualitySafety/TG100/ImplementationGuide.asp from the AAPM Work Group on Implementation of TG 100).

An application of FMEA concepts to EPID dosimetry was published by Bojechko et al. (Bojechko, Phillips et al. 2015), which evaluated the detectability of various radiotherapy errors for pretreatment EPID dosimetry, first fraction transit dosimetry, and all fraction transit dosimetry (Figure 5). They found an advantage in detectability of various failure modes with transit dosimetry versus pretreatment QA. For example, performing first fraction transit dosimetry increased the detectability of several key failure modes relative to pretreatment EPID QA, including wrong isocenter information, patient alignment, and an error in CT scan data, which were some of the most prevalent and potentially severe events studied. By performing transit dosimetry for each treatment fraction, the detectability of patient movement on the table, treatment machine errors, and setup errors is increased. Other EPID dosimetry workflow choices, such as relative vs. absolute dosimetry, may also influence the detectability of errors.

7 KEY RECOMMENDATIONS

The TG-307 report was written to provide guidelines for medical physicists on the commissioning and implementation of EPID-based patient-specific pretreatment and transit dosimetry QA tools. This report focuses on the current commercially available EPID-based PSQA tools and on examples with noncommercial clinical systems which have advanced the application of the use of EPIDs for these applications. The clinical experience of the

TG-307 members along with the extensive published data on EPID QA were used to develop guidelines and provide recommendations on use of EPID-based PSQA methods.

The TG makes the following recommendations:

1. The following information regarding physics, modeling, and algorithm details should be provided by vendors to users: pretreatment and transit dosimetry methods.
    - **a.** The type of physics model used in the EPID system
        - **i.** e.g., providing a comparison of measured EPID gray-level/2D dose distribution with a prediction model
        - **ii.** or extending the calculation of the 2D dose distribution from the image to a 3D dose distribution in a patient geometry using some form of depth-dose modeling
    - **b.** The dosimetric comparison method(s) used
        - **i.** e.g., absolute dose, γ analysis, DVH evaluation
    - **c.** Whether and how the vendor accounts for known needed corrections in EPID systems
        - **i.** central axis position and sag with gantry angle
        - **ii.** uniformity due to flood-field calibration and changes of the uniformity with EPID distance and off-axis positioning
        - **iii.** correction for the support arm backscatter (e.g., Varian aS500 and aS1000 systems)
        - **iv.** whether the vendor scales the image or if the linac manufacturer’s pixel scaling is used
    - **d.** Straightforward access to dosimetrically scaled cine images or preferably individual image frames acquired during VMAT deliveries with the gantry angle interval (and preferably control-point interval) that corresponds to the image provided
        - **i.** clear information from the vendors should be provided stating to what point in the integration time of the image the gantry angle and other information corresponds
        - **ii.** this is to enable more comprehensive QA methods with EPIDs including time-resolved, gantry-resolved, and 3D dose calculation methods if vendors provide such a tool
        - **iii.** for 2D dose images calculated in a phantom, describe the phantom geometry and the depth in phantom where the VMAT dose delivery is calculated

2. Users should be aware of the following implications on clinical use: pretreatment and transit dosimetry methods.
    a. Sensitivity and specificity, and thus alert criteria, are site-specific and depend on the combination of error type and alert indicator (metric) and therefore must be set accordingly by the user, please review section 5.3, where tolerances and alert criteria are more thoroughly discussed
    b. Each institution should assess the sensitivity and specificity of their EPID-based PSQA system to detect errors of different types and magnitude for a set of situations representative of their clinical practice
    c. Users are encouraged to report on their clinical experience with their system with respect to the performance and tolerance levels
        i. these reports may guide other users as to likely performance ranges
        ii. it is expected that differences in performance will be manifested for different centers due to many factors, including the inherent accuracy of planning and delivery of the center as well as the local commissioning of the EPID-based PSQA system
    d. vendors must make publications concerning the sensitivity and specificity as well as the clinical experience with their system available, e.g., on their website
3. Algorithms.
    a. Detailed information on algorithms for these techniques should be published, preferably in peer-reviewed literature. The algorithms used in a forward method, describing the prediction of 2D images or 2D dose distributions at the EPID level, or the algorithm used in a transit back-projection method, yielding single-point (0D), 2D, or 3D dose information in a patient dataset, should be described in detail
    b. Vendors are encouraged to maintain an updated list of these publications on their algorithms freely available, such as on their website
4. Clinical implementation.
    a. Commissioning and calibration
        i. it is recommended that, before a vendor solution is chosen, the user becomes familiar and comfortable with the usability and performance of the system as well as satisfied with the vendor-provided commissioning process
            - Note that the commissioning of a pretreatment IMRT QA system is generally defined by the vendor,

and the user typically does not have the ability to significantly modify the process

ii. commissioning of both the linac and the EPID panel for general imaging use should be completed before the EPID system can be commissioned for pretreatment IMRT QA or transit dosimetry

b. Validation.

i. users should establish a set of validation tests that include a range of delivery patterns to measure and verify the accuracy of the system and generate a baseline for periodic QA and system maintenance. Review section 5 for specific validation and QA tests and recommendations

ii. users should induce errors of known magnitude to validate that the PTQA and transit dosimetry system are operating as expected and are sensitive to clinically relevant errors. Sections 4 and 5 provide specific examples of induced errors for testing purposes and validation

c. Routine QA of EPID systems

i. all periodic checks of the EPID-based PSQA system should be performed based on the recommendations given in Table 6

d. Expectations regarding tolerance levels for PSQA

i. the passing criteria for PTQA should be the same as or similar to that achieved with other detector arrays, typically greater than 95% of pixels passing 3%G/2 mm with a 10–20% dose threshold

ii. for 2D relative mode transit γ analysis, the passing criteria and tolerances should be the same as or similar to the PTQA, such as greater than 95% γ passing rate with 3%G/2 mm

iii. for 2D absolute dose mode transit dosimetry, the criteria and tolerance may be looser due to the uncertainties of the dose conversion from the EPID image pixel data

- the user should base the choice of acceptable γ passing rate both on what was achievable during commissioning and what others have reported in the literature (see Tables 7 and 8)

iv. the tolerance of the 3D γ analysis for PTQA with EPID-based solutions should generally be the same as for the standard 2D and 3D detector arrays, following TG 218 guidelines

v. as with EPID-based 2D transit dosimetry, reconstructed 3D dose should be compared with a well-established dosimetric method, such as the TPS dose in the planning CT using an inhomogeneous phantom (with film or individual detector measurements for further independent verification). If a system performs the back-projection on CBCTs, then a separate intercomparison should be made using the same phantom to evaluate the accuracy of handling the potentially smaller field of view, Hounsfield Unit to relative electron density conversion, and artifacts in the CBCT

vi. where the OAR dose is close to known safe tolerance values, the physicist should alert the radiation oncologist to carefully consider what to allow during daily QA

vii. if the magnitude of the error is clinically significant after considering any patient-specific considerations, then the physicist should attempt to determine the reason(s) for the failure

5. Risk-based analysis.

   a. Clinics implementing EPID dosimetry should use risk-based QA tools, such as FMEA and incident learning, to continuously review and improve the efficacy of the program

   b. This TG encourages EPID dosimetry users to revisit existing QA processes in the clinic and their prior FMEA efforts to assess the impact on quality and safety of the increased error detectability afforded by these systems

8 NEW DEVELOPMENTS

Several notable new developments in the use of EPID that are outside the scope of this report which focuses on commercially available tools are worthwhile briefly mentioning here. Artificial intelligence and machine learning techniques have recently been investigated to classify error types in IVD QA results (Wolfs, Canters et al. 2020). Methods to include uncertainty analysis for EPID dosimetry calculation models are also of interest (Baeza, Wolfs et al. 2018). Valdes et al. developed a machine learning algorithm to correlate the characteristics of IMRT plan and delivery characteristic and the corresponding gamma passing rate for a variety of QA devices (Valdes, Chan et al. 2017). A work by Zhang et al. describes the development of a predicted EPID transmission image using Monte Carlo and deep learning algorithms for potential use for *in vivo* treatment verification (Zhang, Cheng et al. 2022). Nyflot et al. investigated a deep learning approach to classify the presence or absence of intentionally introduced treatment delivery errors from IMRT PSQA (Nyflot, Thammasorn et al. 2018). Their results demonstrated that the performance of the deep learning network was superior to a handcrafted radiomic approach. Another work by Lam et al. applied multiple tree-based machine learning-based methods to predict the gamma pass

rates for portal dosimetry based IMRT PSQA (Lam, Zhang et al. 2019). Such machine-based methods may be used to better identify the IMRT QA failures and to develop proactive QA approaches.

9 CONCLUSIONS

EPID-based QA has matured and is widely used in clinical practice for verification of accurate dose delivery. The proposed recommendations in this report were written to ensure the proper implementation of EPID-based QA tools for patient-specific IMRT/VMAT QA. The report provides information about commercially available EPID QA solutions known at the time of writing the report; a review of EPID technology, physics, modeling, and algorithms used for EPID dosimetry; and clinical use of pretreatment and transit dosimetry techniques, limitations, and challenges. It provides recommendations on the commissioning, calibration, routine QA, risk-based analysis for EPID QA systems. At the end, the report recommends the tolerance levels for PSQA using commercially available EPID based QA systems for both pretreatment and transit dosimetry.

ACKNOWLEDGMENTS

The authors would like to thank Jennifer Clark from Sun Nuclear for her thorough review and comments on this report. Jean Moran acknowledges support from the NIH/NCI Memorial Sloan Kettering Cancer Center (MSK) Support Grant (P30 CA008748).

APPENDIX A: ALGORITHMS: PRETREATMENT VERIFICATION METHODS

A.1 Portal Dosimetry (Varian Medical Systems)

This method derives a prediction of the EPID image to compare with the measured image. The delivery at the linac uses a separate Portal Dosimetry plan; The predictions and comparisons are based on integrated images. For VMAT, it is possible to split the VMAT arc into several smaller subarcs of arbitrary angle subtended, which become separate deliveries with an integrated image acquired for each subarc. This involves a slight change in the delivery from the original arc as the beam is shut off and restarted to deliver each subarc.

The prediction model is an analytical model developed by van Esch et al. (Van Esch, Depuydt et al. 2004). The predicted intensity in calibrated units (CUs) per MU is expressed using the equation:

$$\mathrm{PD}(x, y, \mathrm{SDD}) = [F(x, y, \mathrm{SDD}) \cdot \mathrm{OAR}(\mathrm{SDD}) \otimes \mathrm{RF}_{\mathrm{PI}}] \cdot \mathrm{CSF}_{XY} \cdot \frac{1}{\mathrm{MU\ factor}},$$

where $F(x, y, \mathrm{SDD})$ is an incident fractional beam-on fluence model, OAR is an entered off-axis ratio profile, RF is an EPID scatter kernel, CSF_{XY} is a field-size dependent correction factor. The kernel parameters are either determined using optimization to a measured image and measurement of CSF_{XY} are obtained by the user, or the user can be provided with generic (preconfigured) model parameters. More recently, Varian has modified the AAA algorithm to calculate EPID image signals. The system includes calibrations applied automatically to the measured EPID images. A calibration to CU, based on a $10 \times 10\ \mathrm{cm}^2$ delivery and

specified CU value by the user and a 2D matrix correction, is applied to the image. The correction matrix was originally used to add a dose in water beam profile back to the image as beam profiles are flattened due to the flood-field correction image applied. More recently, it has been adapted to provide a correction to the backscatter component of the flood-field image due to the Varian support arm which rests underneath the active detector layers.

A.2 Adaptivo (Standard Imaging)

Adaptivo pretreatment is a portal image prediction algorithm that predicts CU for Varian systems. The EPID is calibrated according to the Varian Portal Dosimetry procedure. Adaptivo performs additional calibrations where a PSM is determined using user measurements. This is applied to the measured image by first removal of the Varian applied flood-field followed by application of the PSM. This allows for EPID movement off axis when required. The result is an image which represents the inherent EPID response to the beam including the energy dependence. EPID arm backscatter is also present in this image. The backscatter component of the measured image is also corrected using an empirical method (Berry, Polvorosa et al. 2010). The prediction algorithm models the EPID response using a fluence matrix (open density matrix) derived from the MLC control points that is convolved with energy-dependent EPID dose-deposition kernels. The off-axis fluence profile and off-axis beam softening is included in the model.

A.3 SOFTDISO (Best NOMOS)

A pre-treatment option is provided to compare a normalized fluence map derived from the treatment plan with a normalized EPID image. The fractional MU value is combined with the MLC aperture for each control point to create a binary fluence. These are summed over all control points to create a map that represents the fractional MU delivered to each point, sometimes referred to as the opening density matrix. Then the map is normalized to the maximum value. EPID images are also normalized to the maximum value—there is no dose conversion. It is intended to find any leaf movement fail, not a full dosimetric validation of the fluence.

A.4 Epiqa (EPIdos)

This method converts the EPID image to a dose plane in a virtual slab water phantom. The method was originally developed by Nicolini et al. (Nicolini, Fogliata et al. 2006) and termed the GLAaS algorithm. The method is based on a series of linear curves that relate EPID pixel value to dose in water as a function of field size for both primary beam (*pr*) and MLC transmitted beam (*tr*). It accounts for the difference in EPID response to open and MLC transmitted beam, which is approximately 30% (Li, Siebers et al. 2006):

$$D_{pr} = m_{pr}(EwwF) \cdot P_{pr} + q_{pr}(EwwF), \quad D_{tr} = m_{tr}(EwwF) \cdot P_{tr} + q_{tr}(EwwF),$$

where D is the dose in Gy measured in a water phantom ($d_{\max}$) with ion chamber at the center of the square field, $EwwF$ is the field size, P is the mean pixel value for a region of interest at the center of the field, and m and q, which are both a function of the field size, are the

fitted linear parameters with $q \sim 0$. From the MLC plan file, the primary signal P_{pr} to each pixel from each MLC segment is estimated so that the above calibration curves can then be applied by summing the contributions of each segment. The transmission signal for each pixel is estimated from the estimated primary signal subtracted from the measured signal, and the transmission dose is estimated from the above equation.

A.5 EPIbeam (DOSIsoft)

This method converts the EPID image to a dose plane in a virtual slab water phantom. Currently, the reference dose plane at 5 cm depth in the water slab is calculated by the EPIbeam software using the exported DICOM treatment plan. For a Varian system with support arm backscatter, a backscatter kernel method is used to predict and subtract backscatter from both the measured image and the flood-field correction image. This uses masking of the images to give the component of the image irradiating the support arm followed by convolution of the image with a backscatter kernel (Rowshanfarzad, McCurdy et al. 2010). The flood-field correction applied to the measured image is first removed. Then the backscatter removed image is divided by the backscatter removed flood-field image. A ghosting response factor is also applied to correct nonlinearity of response with MU:

$$\mathrm{Dose}(\mathrm{x},\ \mathrm{y}) = \mathrm{CF} \cdot t\mathrm{EPI}(\mathrm{x},\ \mathrm{y}) \cdot \mathrm{BP}(\mathrm{x},\ \mathrm{y}) \otimes^{-1} \mathrm{KF} \otimes \mathrm{KP}\,.$$

Calculating the dose in water involves multiplication of the above corrected image ($t\mathrm{EPI}(\mathrm{x}, \mathrm{y})$) by a calibration factor (CF), a 2D beam profile matrix $\mathrm{BP}(\mathrm{x}, \mathrm{y})$, deconvolution with a silicon to water kernel (KF), and convolution with a beam penumbra in water kernel (KP). The dose model is calibrated using the raw computed value for a 10×10 cm^2 field and the known dose for the field.

A.6 EPIDose (Sun Nuclear)

This method converts the EPID image to a dose plane in a virtual slab water phantom. The following description is from a paper published by Bailey et al. (Bailey, Kumaraswamy et al. 2012). The EPIDose software converts EPID images via a four-step algorithm: (1) image back-projection accounting for divergence of the beam between the SDD and desired source-dose plane distance; (2) output factor matrix accounting for variation in EPID response to field size (i.e., effective field size of each segment for IMRT fields) and MLC transmission; (3) dose redistribution via a point-spread kernel which converts measured EPID response to relative dose response at depth in water; and (4) a 2D conversion from relative to absolute dose response for each pixel. All beam data are acquired by measuring commissioning fields with the MapCHECK diode array. Thus, EPIDose-calculated dose planes can be directly compared with TPS calculated dose planes (at specified depth in water), providing an independent additional check of the actual TPS dose calculation algorithm. The EPIDose physics modeling process allows optimization of the EPID physics model to best match similar EPIDose-calculated and MapCHECK-measured dose planes.

A.7 PerFRACTION—SunCHECK Patient (Sun Nuclear)

A.7.1 2D Option

This method converts an EPID image to a dose plane in a virtual slab water phantom at a depth of 5 cm. The reference dose plane in the water slab is calculated by the SDC using the DICOM treatment plan. A description of and validation of the algorithm has been provided by Ahmet, Hunt et al. (Ahmed, Hunt et al. 2017). It is a calibration-based approach where the EPID signal-to-dose conversion factors are stored in a look-up matrix. These are derived from a calibration procedure involving irradiation of a number (the exact number depends on the EPID imager model and SID) of rectangular fields of varying widths and positions to the EPID in air. The conversion factors are created as follows: for each pixel, absolute dose = conversion matrix (P, EFS, P_{ratio}) * EPID response, where P = pixel position, EFS = effective field size, and P_{ratio} = primary signal ratio.

For each field or arc in a patient plan, these conversion factors are precalculated: at each pixel position the P_{ratio} and effective field width from each segment of the beam are determined, along with radiological path length (via ray trace) and expected detector distance. The relevant conversion factor for each control point is then extracted from the calibration matrix. A weighted mean of the conversion factors over all segments for each pixel is calculated and the result is stored in the SunCHECK database. After EPID acquisition, each pixel can be rapidly converted to water-equivalent dose values by application of the stored conversion factors.

A.7.2 3D Option (Non Dosimetric)

3D reconstruction in SunCHECK Patient (PerFRACTION) is a forward-projection calculation that uses a combination of cine EPID images and log files, named EpiLog method. The frames of cine EPID images are used to detect MLC leaf and collimator positions over time, which are synchronized with gantry angle, dose rate, and MU information from the log file. These delivery parameters are then used to recalculate dose in the patient geometry (planning CT or CBCT) using the SDC as described below in transit dosimetry methods. Note: the 3D reconstruction is independent of the 2D method above; no dosimetric information is derived from the EPID image for the purposes of 3D calculation. Only the field shape/MLC leaf tip positions are derived for each frame of the cine image.

A.8 RadCalc EPID (LAP)

Formerly known as the DosimetryCheck system. To obtain the incident fluence model from the EPID image, EPID scatter kernel parameters were optimized to minimize the variance between measured dose profiles in a water tank and EPID derived dose (Renner, Norton et al. 2005). The beam profile “horns” that are removed by the EPID flood-field calibration procedure are restored to the resulting images by direct multiplication using the measured in-air, off-axis ratio.

The dose calculation in the patient dataset is a pencil beam superposition model. For dose calculation in the patient, the pencil beam kernel is first stretched or compressed according to the radiological depth along the central ray of each pencil beam to obtain the dose

distributions of each pencil beam in the patient. This achieves a first-order approximation to account for the effects of inhomogeneities in the patient. These location-specific pencil beam dose distributions are then weighted by the intensity values derived at each pencil beam location from the measured fluence map and superimposed to get the dose distribution of the broad beam.

A.9 3DVH (Sun Nuclear)

3DVH imports the 2D dose distribution per IMRT field from EPIDose (section A.1.7) to reconstruct all the fields into a 3D dose distribution in patient. 3DVH uses the ratio of the planar dose in phantom to the TPS expected dose in water at the same plane. The resulting "perturbation matrix" is then back-projected divergently through the original TPS planned dose in patient to yield an estimate of 3D delivered dose for each field. The perturbed doses for all fields are added together to form a composite dose volume in patient geometry. DVH analysis is then performed comparing the planned dose with the perturbed "delivered" dose.

APPENDIX B: ALGORITHMS: TRANSIT (IN VIVO) DOSIMETRY METHODS

B.1 PerFRACTION—SunCHECK Patient (Sun Nuclear)

B1.1 2D Option

The 2D transit dosimetry approach follows the method for 2D pretreatment verification as described above. The conversion of EPID response to dose requires a calibration procedure to be performed in advance, resulting in the creation of a signal-to-dose calibration matrix. The delivery of varying widths and positions of rectangular fields is like the pretreatment calibration process but also includes deliveries through 30 and 10 cm of Solid Water™ in addition to a reduced number of in-air measurements. The predicted dose image for each field is generated by projecting the planned beams through the patient's planning CT dataset and calculating the resultant transit dose to a virtual water slab at the plane of the EPID at a depth of 2.5 cm. The measured EPID data converted to water-equivalent absolute dose can then be compared with this calculated predicted dose image as early as the first fraction delivery. Note that comparison of the measured EPID dose distribution to a TPS-generated 2D dose map is not currently possible within SunCHECK but may be accomplished by exporting the dose maps from both SunCHECK and TPS and using another software application such as SNC Patient.

B1.2 3D Option

The 3D dose distribution is reconstructed in the patient dataset (planning CT or CBCT) via forward projection using delivery information from the machine log files and/or detected MLC and collimator positions from cine EPID imaging like the pretreatment 3D dose calculation described above. The SDC algorithm here consists of three steps: a fluence calculation using a dual source model for radiation transport within the accelerator head, an inverse TERMA calculation for radiation transport from the accelerator to the patient, and a superposition (using an inverse superposition kernel and collapsed cone approximation) for radiation transport within the patient. CBCT images are fused with the planning CT using rigid registration from the DICOM registration object, and a CBCT-specific electron density

table is applied. This allows changes in patient positioning or anatomy to be reflected in the 3D dose distribution, although the DVH results are still based on the original planning contours. Note that the 3D reconstruction is independent of the 2D method above; no transit dosimetric information is currently derived from the EPID image for the purposes of 3D calculation.

B.2 Adaptivo (Standard Imaging)

A pencil beam algorithm is used to predict the EPID image in CUs. Predicted transit images account for beam attenuation based on the planning CT. The daily couch position can be accounted for automatically in the predicted attenuation calculation. Comparison of the measured EPID dose distribution with a TPS-generated 2D dose map is not possible. More information about the Adaptivo algorithm can be found in the new Section A.2 (Section 1.6 in the old version).

B.3 EPIgray (DOSIsoft)

The prediction model of EPIgray is an empirical model developed by François et al. (Francois, Boissard et al. 2011). After calibrating the EPID, several conversion factors are required to obtain the dose reconstructed in the patient as illustrated in Figure B1.

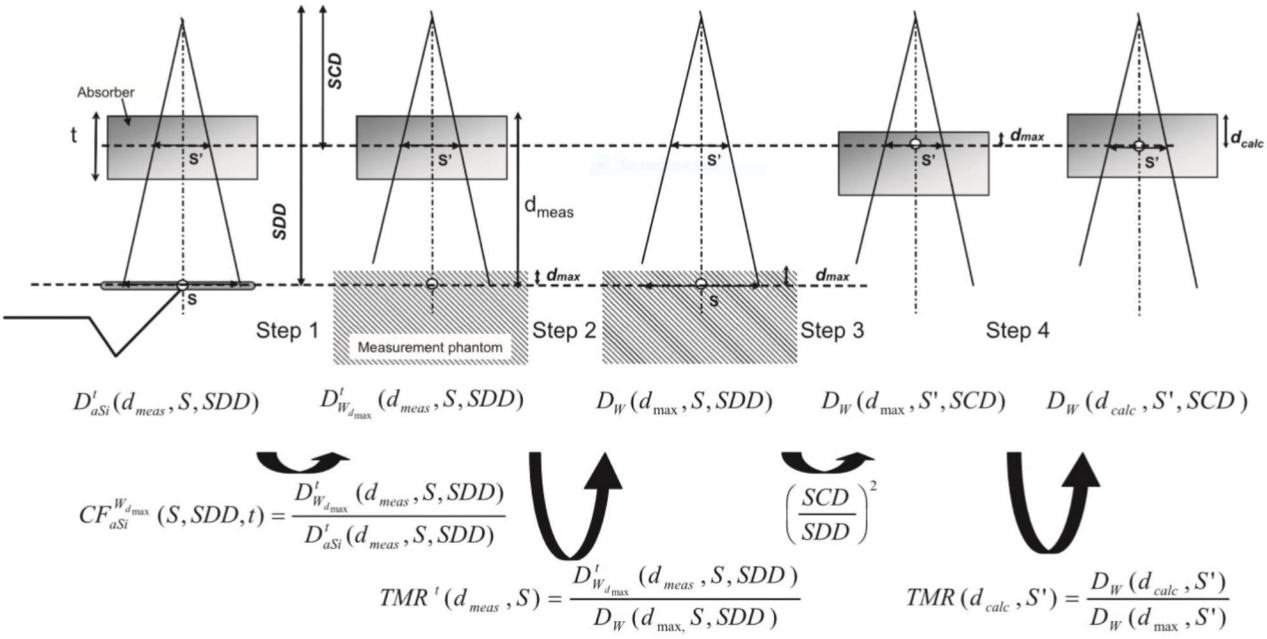

Figure B1.
The formalism for back-projection of a transit dose measured with an EPID to determine the dose within the patient as used in EPIgray. Steps 2–4 can be used with any type of detector (reproduced from Francois, Boissard et al. 2011).

For this purpose, a series of phantom measurements must be performed for a range of setups with different field sizes, phantom thicknesses, and source-to-phantom-surface distances. The conversion factors *FC* are then calculated according to

$$FC = \frac{D_{TPS}}{D_{calib} \times CU} \times \left(\frac{SID}{SAD}\right)^2 \times \frac{fTMR_{(phantom\_thickness)}}{TMR_{(isocenter\_depth)}},$$

where D_{TPS} is the dose calculated by the TPS at isocenter, D_{calib} is the calibration dose at D_{max} for 100 MU delivered by a 10 × 10 cm^2 field size and a 100 cm SAD setup, CU is the calibration unit read out from the portal image, and $\left(\frac{SID}{SAD}\right)^2$ is the inverse square distance correction from the SID at the isocenter. The term $\times \frac{fTMR_{(phantom\_thickness)}}{TMR_{(isocenter\_depth)}}$ is included to calculate the dose at isocenter for various phantom thicknesses. Here, $fTMR_{(phantom\text{-}thickness)}$ is the finite tissue-maximum ratio, which is the ratio between two doses measured in a phantom at the EPID level at the depth of D_{max} under the same conditions with and without a finite phantom of a specific thickness in the beam. Also, $TMR_{(isocenter\text{-}depth)}$ is the tissue-maximum ratio required to calculate the dose at the depth of the isocenter or other point of interest. The dose conversion model of the portal images includes the EPID sag effect and the dose calibration factor, which results in dose values expressed in cGy.

B.4 SOFTDISO (Best Medical)

The empirical dose reconstruction algorithm of SOFTDISO is based on the correlation between the EPID transit signal and the dose measured along the central beam axis in a solid water phantom in the phantom midplane for different phantom thicknesses and field sizes, as illustrated in Figure B2.

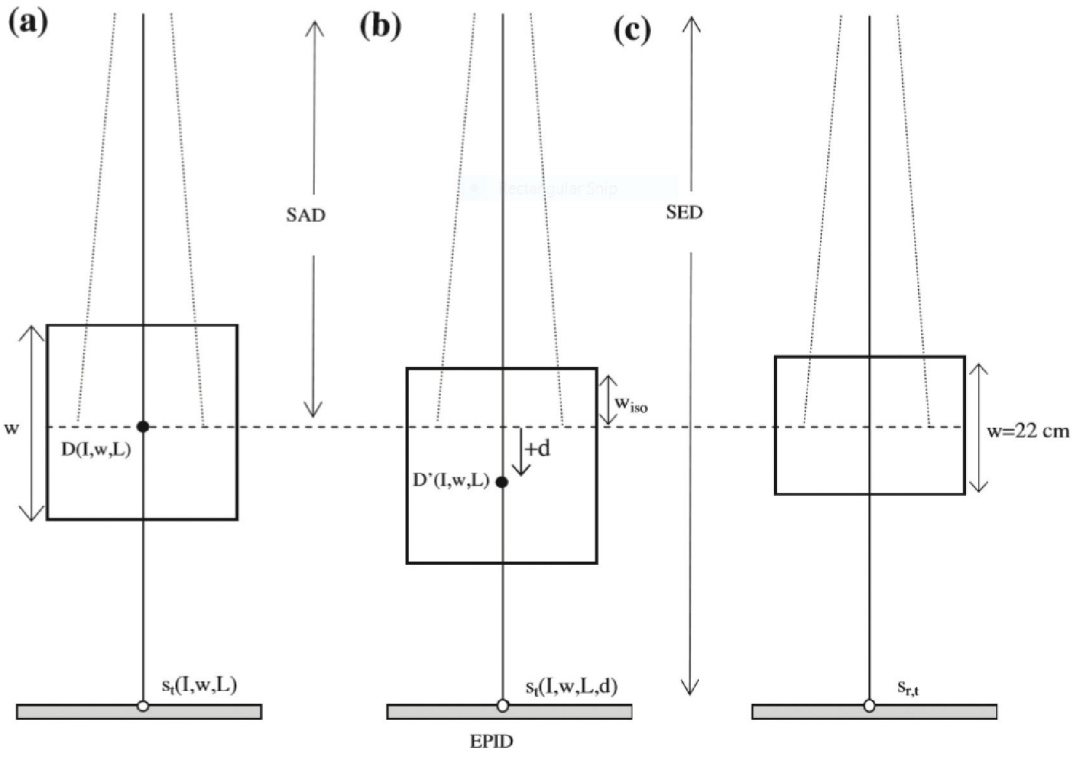

Figure B2.

Schematic diagram of a solid water phantom of thickness w irradiated by square open or wedged fields L × L in size. The EPID is positioned at the SID to measure the transit signals $s_t(\mathrm{I}, w, \mathrm{L})$ and $s_t(\mathrm{I}, w, \mathrm{L}, d)$ at point s. (a) Reference configuration with an IC positioned in the midplane at SAD = 100 cm to determine the midplane dose $D(\mathrm{I}, w, \mathrm{L})$. (b) The midplane is positioned at the distance d below the SAD to determine the midplane dose $D'(\mathrm{I}, w, \mathrm{L})$. (c) A phantom with w = 22 cm is irradiated to obtain a reference transit signal $s_{r,t}$ required for the determination of the calibration factor k_s (reproduced from Piermattei, Greco et al. 2012).

The dose values and the transit signals are fitted by polynomial functions. The transit isocenter dose D_{iso} can then be obtained by multiplying the EPID transit signal with an overall correlation function that considers all treatment and patient parameters, such as field dimension, patient radiological thickness, beam energy, isocenter depth, number of MU, and other factors. A software package SOFTDISO connected with the record and verify system is used to determine the parameters required for the determination of the overall correlation factor using the DICOM files supplied by the CT scanner and the TPS. The software commissioning requires measurements for each beam of the beam quality index $\mathrm{TPR}_{20,10}$, the beam output factor, both determined during the linac commissioning and periodically verified, the EPID calibration factor, and its dependence on the number of MU used. The mathematical aspects of the dose reconstruction algorithm have been discussed by the Italian group in several papers (Fidanzio, Porcelli et al. 2014, Cilla, Meluccio et al. 2016, Falco, Giancaterino et al. 2018) and summarized in Section B4. A second module is used to perform a γ analysis of the day-to-day EPID images as discussed in Section 3.2.1.

B.5 RadCalc EPID (LAP)

Formerly known as the DosimetryCheck system, the RCE software has two main components. The first concerns a mapping between the EPID fluence and the number of MU that would produce the same fluence at the center of a 10 × 10 cm^2 field at the appropriate reference conditions. The output of this mapping is termed the relative MU (RMU). It also considers the scatter within the EPID housing (by deconvolution of the EPID fluence) as well as the scattered radiation reaching the EPID from the presence of a patient in the beam. To account for points not on the central axis, the in-air, off-axis ratio along the diagonals of a 40 × 40 cm^2 field is used. From the knowledge of the fluence at each pixel of the EPID in RMU, the beam geometry, and the patient CT, it is possible to ray-trace from the x-ray source through the equivalent thickness of water that would produce this fluence. The same principle is applied when the planning CT is used in place of water, and ray-tracing is used to establish the dose at a point in the CT and hence the patient. The fluence map collected by the EPID image is the source of input for the RCE pencil beam dose calculation engine. The dose distribution calculated by RCE is then compared with the dose matrix calculated by the TPS. Quantitative evaluation of the difference between the planned and measured dose distribution is carried out in RCE by point dose comparison or by using 3D γ or dose-volume analysis.

B.6 iViewDose (Elekta)

The iViewDose transit dose reconstruction algorithm is schematically shown in Figure B3.

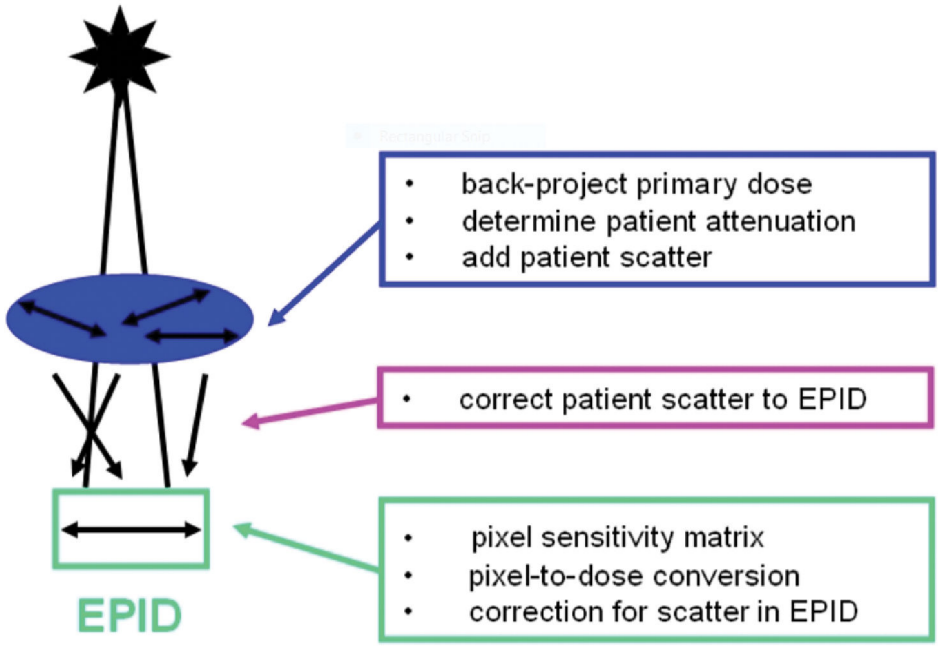

Figure B3.
Schematic presentation of the various steps involved in the reconstruction of the dose distribution inside a patient/phantom from an EPID measurement using the iViewDose back-projection model (reproduced from Mijnheer, Olaciregui-Ruiz et al. 2013).

It requires the primary dose distribution at the EPID level $\mathrm{Pr}_{ij}^{\mathrm{EPID}}$ for a certain pixel ij. This is calculated from the pixel values $PV_{ij}^{\mathrm{EPID,patient}}$ of EPID images and/or frames measured behind the patient (or phantom) after correcting for the sensitivity matrix S_{ij}, applying the EPID dose response D_r, removing the scatter within the EPID by deconvolving with kernel K_{ij}^{EPID1} and blurring the EPID signal with convolution kernel K_{ij}^{EPID2}, correcting for the couch attenuation C_{ij}, and removing the scatter from the patient to the EPID using $SC_{ij}^{\mathrm{patient,EPID}}$:

$$Pr_{ij}^{\mathrm{EPID,\ patient}} = \left(\left(PV_{ij}^{\mathrm{EPID,transit}} \cdot S_{ij} \cdot D_r\right) \otimes^{-1} K_{ij}^{\mathrm{EPID1}} \otimes K_{ij}^{\mathrm{EPID2}}\right) \cdot C_{ij} \cdot SC_{ij}^{\mathrm{patient,EPID}}.$$

The primary dose in a patient $P_{ij}(d_{\mathrm{reconst}})$ at a point at a distance d_{reconst} of the reconstruction plane from the accelerator target is derived from $\mathrm{Pr}_{ij}^{\mathrm{EPID}}$ by means of:

$$\mathrm{Pr}_{ij}(d_{\mathrm{reconst}}) = \mathrm{Pr}_{ij}^{\mathrm{EPID}} \cdot \left(\frac{d_{\mathrm{reconst}}}{d_{\mathrm{EPID}}}\right)^{-2} \cdot AC_{ij}(d_{\mathrm{reconst}}),$$

where d_{EPID} is the distance of the EPID from the accelerator target and $(d_{\mathrm{reconst}}/d_{\mathrm{EPID}})^{-2}$ is a scaling factor representing the inverse-square law. The attenuation correction AC_{ij} considers the attenuation of the primary dose between the reconstruction plane and the EPID. Finally, the total dose at depth d_{reconst} in the patient is calculated by adding the patient-specific scatter component to the primary dose at that point. The 3D model is an iteration of these calculations in multiple planes parallel to the EPID within the patient volume. Full details

regarding the physics model can be found in Wendling et al. (Wendling, McDermott et al. 2009) and its adaptation for VMAT verification in Mans et al. (Mans, Remeijer et al. 2010).

Glossary

0D	zero dimensional
2D	two dimensional
3D	three dimensional
3DCRT	3D conformal radiation therapy
a-Si	amorphous silicon
AAPM	American Association of Physicists in Medicine
ART	adaptive radiotherapy
CCD	charge-coupled device
CBCT	cone-beam computed tomography
CT	computed tomography
CU	calibrated unit
DICOM	Digital Imaging and Communications in Medicine
DIR	deformable image registration
DPS	dosimetric pixel scaling
DVH	dose-volume histogram
EPID	electronic portal imaging device
ESTRO	European Society for Radiotherapy and Oncology
FFF	flattening filter free
FMEA	failure modes and effects analysis
H&N	head and neck
HIS	Heimann imaging software
HU	Hounsfield unit
IC	ion chamber
ILS	incident learning system
IMRT	intensity modulated radiation therapy
IPS	image processing service

JPEG	Joint Photographic Experts Group
IVD	*in vivo* dosimetry
Linac	linear accelerator
MLC	multileaf collimator
MU	monitor unit
OAR	organ at risk
PC	perpendicular composite
PFF	perpendicular field-by-field
PSM	pixel sensitivity map
PSQA	patient-specific quality assurance
PTQA	pretreatment quality assurance
PTV	planning target volume
QA	quality assurance
RCE	RadCalc EPID (formerly Dosimetry Check)
RO-ILS	Radiation Oncology Incident Learning System
ROC	receiver operating characteristic
RPN	relative priority number
SBRT	stereotactic body radiation therapy
SD	standard deviation
SDC	Sun Nuclear Dose Calculator
SDD	source-detector distance
SID	source-imager distance
SPD	source-dose plane distance
SRS	stereotactic radiosurgery
TPS	treatment planning system
XML	Extensible Markup Language
VMAT	volumetric modulated arc therapy

REFERENCES

Adamson J, Wu Q. Independent verification of gantry angle for pre-treatment VMAT QA using EPID. Phys Med Biol. 2012; 57:6587–6600. [PubMed: 23010739]

Ahmed S, Hunt D, Kapatoes J, Hayward R, Zhang G, Moros EG, Feygelman V. Validation of a GPU-Based 3D dose calculator for modulated beams. J Appl Clin Med Phys. 2017;18 (3):73–82. [PubMed: 28371377]

Alhazmi A, Gianoli C, Neppl S, et al. A novel approach to EPID-based 3D volumetric dosimetry for IMRT and VMAT QA. Phys Med Biol. 2018; 63:115002. [PubMed: 29714714]

Ansbacher W Three-dimensional portal image-based dose reconstruction in a virtual phantom for rapid evaluation of IMRT plans. Med Phys. 2006; 33:3369–3382. [PubMed: 17022233]

Antonuk L Future EPID technology and applications. Med Phys. 2016; 43:3745–3745.

Antonuk LE, Boudry J, Huang WD, et al. Demonstration of megavoltage and diagnostic-x-ray imaging with hydrogenated amorphous-silicon arrays Med Phys 1992;19:1455–1466. Med Phys. 1993; 20:825–825.

Antonuk LE, Yorkston J, Huang W, et al. A real-time, flat-panel, amorphous silicon, digital x-ray imager. Radiographics. 1995; 15:993–1000. [PubMed: 7569143]

Antonuk LE, Yorkston J, Huang WD, Sandler H, Siewerdsen JH, ElMohri Y. Megavoltage imaging with a large-area, flat-panel, amorphous silicon imager. Int J Radiat Oncol Biol Phys. 1996; 36:661–672. [PubMed: 8948351]

Baeza AB, Wolfs CJA, Nijsten SMJJG, Verhaegen F. Validation and uncertainty analysis of a pre-treatment 2D dose prediction model. Phys Med Biol. 2018; 63(3):1–13.

Bailey DW, Kumaraswamy L, Bakhtiari M, Malhotra HK, Podgorsak MB. EPID dosimetry for pretreatment quality assurance with two commercial systems. J Appl Clin Med Phys. 2012; 13:82(4);82–99.

Bailey DW, Kumaraswamy L, Podgorsak MB. An effective correction algorithm for off-axis portal dosimetry errors. Med Phys. 2009; 36:4089–4094. [PubMed: 19810481]

Barbeiro AR, Parent L, Younes T, et al. Dosimetric response of aSi1000 EPID continuous imaging of FFF beams for in vivo 3D SBRT verification. Radiother Oncol. 2019;133: S920–S920.

Ballangrud A, Kuo LC, Happersett L, et al. Institutional experience with SRS VMAT planning for multiple cranial metastases. J Appl Clin Med Phys. 2018;19(2):176–183. [PubMed: 29476588]

Bedford JL, Hanson IM. A method to verify sections of arc during intrafraction portal dosimetry for prostate VMAT. Phys Med Biol. 2019; 64:205009. [PubMed: 31553964]

Bedford JL, Hanson IM, Hansen VN. Portal dosimetry for VMAT using integrated images obtained during treatment. Med Phys. 2014; 41:021725. [PubMed: 24506616]

Bedford JL, Hanson IM, Hansen VN. Comparison of forward- and back-projection in vivo EPID dosimetry for VMAT treatment of the prostate. Phys Med Biol. 2018; 63:025008. [PubMed: 29165319]

Berry SL, Polvorosa CS, Wuu CS. A field size specific backscatter correction algorithm for accurate EPID dosimetry. Med Phys. 2010; 37:2425–2434. [PubMed: 20632552]

Blake SJ, McNamara AL, Deshpande S, et al. Characterization of a novel EPID designed for simultaneous imaging and dose verification in radiotherapy. Med Phys. 2013;40(9):091902. [PubMed: 24007153]

Blake SJ, Vial P, Holloway L, Greer PB, McNamara AL, Kuncic Z. Characterization of optical transport effects on EPID dosimetry using Geant4. Med Phys. 2013; 40:1–14.

Bojechko C, Ford EC. Quantifying the performance of in vivo portal dosimetry in detecting four types of treatment parameter variations. Med Phys. 2015; 42:6912–6918. [PubMed: 26632047]

Bojechko C, Phillips M, Kalet A, Ford EC. A quantification of the effectiveness of EPID dosimetry and software-based plan verification systems in detecting incidents in radiotherapy. Med Phys. 2015; 42:5363–5369. [PubMed: 26328985]

Bossuyt E, Weytjens R, Nevens D, De Vos S, Verellen D. Evaluation of automated pre-treatment and transit in-vivo dosimetry in radiotherapy using empirically determined parameters. Phys Imaging Radiat Oncol. 2020; 16:113–129. [PubMed: 33458354]

Bresciani S, Poli M, Miranti A, et al. Comparison of two different EPID-based solutions performing pretreatment quality assurance: 2D portal dosimetry versus 3D forward projection method. Phys Med. 2018; 52:65–71. [PubMed: 30139611]

Cai B, Goddu SM, Yaddanapudi S, et al. Normalize the response of EPID in pursuit of linear accelerator dosimetry standardization. J Appl Clin Med Phys. 2018;19(1):73–85. [PubMed: 29125224]

Celi S, Costa E, Wessels C, Mazal A, Fourquet A, Francois P. EPID based in vivo dosimetry system: clinical experience and results. J Appl Clin Med Phys. 2016;17(3):262–276.

Childress NL, Salehpour M, Dong L, et al. Dosimetric accuracy of Kodak EDR2 film for IMRT verifications. Med Phys. 2005; 32:539–548. [PubMed: 15789600]

Chendi A, Botti A, Orlandi M, et al. EPID-based 3D dosimetry for pre-treatment FFF VMAT stereotactic body radiotherapy plan verification using dosimetry CheckTM. Phys. Med 2021; 81:227–236. [PubMed: 33485140]

Chuter RW, Rixham PA, Weston SJ, Cosgrove VP. Feasibility of portal dosimetry for flattening filter-free radiotherapy. J Appl Clin Med Phys. 2016;17(1):112–120.

Cilla S, Meluccio D, Fidanzio A, et al. Initial clinical experience with Epid-based in-vivo dosimetry for VMAT treatments of head-and-neck tumors. Phys Med. 2016; 32:52–58. [PubMed: 26511150]

Cilla S, Azario L, Greco F, et al. An in-vivo dosimetry procedure for Elekta step and shoot IMRT. Phys Med. 2014; 30:419–426. [PubMed: 24361278]

Colodro JFM, Berna AS, Puchades VP, Amores DR, Banos MA. Volumetric-modulated arc therapy lung stereotactic body radiation therapy dosimetric quality assurance: a comparison between radiochromic film and chamber array. J Med Phys. 2017; 42:133–139. [PubMed: 28974858]

Consorti R, Fidanzio A, Brainovich V, et al. EPID-based in vivo dosimetry for stereotactic body radiotherapy of non-small cell lung tumors: Initial clinical experience. Phys Med. 2017; 42:157–161. [PubMed: 29173910]

Covington EL, Synder JD, Wu X, Cardan R, Popple RA. Assessing the feasibility of single target radiosurgery quality assurance with portal dosimetry. J Appl Clin Med Phys. 2019;20(5):135–140.

El-Mohri Y, Antonuk LE, Yorkston J, et al. Relative dosimetry using active matrix flat-panel imager (AMFPI) technology. Med Phys. 1999; 26:1530–1541. [PubMed: 10501053]

Esposito M, Bruschi A, Bastiani P, et al. Characterization of EPID software for VMAT transit dosimetry. Australas Phys Eng Sci Med. 2018; 41:1021–1027. [PubMed: 30341673]

Esposito M, Ghirelli A, Pini S, et al. Clinical implementation of 3D in vivo dosimetry for abdominal and pelvic stereotactic treatments. Radiother Oncol. 2021; 154:14–20. [PubMed: 32926910]

Esposito M, Marrazzo L, Vanzi E, et al. A Validation for EPID In Vivo Dosimetry Algorithms. Appl Sci. 2021; 11:1–10.

Essers M, Boellaard R, vanHerk M, Lanson H, Mijnheer B. Transmission dosimetry with a liquid-filled electronic portal imaging device. Int J Radiat Oncol Biol Phys. 1996; 34:931–941. [PubMed: 8598373]

Falco MD, Giancaterino S, De Nicola A, et al. In-vivo dosimetry: a feasibility study in routine clinical practice. Radiother Oncol. 2018;127: S941–S941.

Fidanzio A, Porcelli A, Azario L, et al. Quasi real time in vivo dosimetry for VMAT. Med Phys. 2014; 41:062103. [PubMed: 24877830]

Fidanzio A, Azario L, Greco F, et al. Routine EPID in-vivo dosimetry in a reference point for conformal radiotherapy treatments. Phys. Med. Biol. 2015;60(8):N141–N150. [PubMed: 25826045]

Fogliata A, Clivio A, Fenoglietto P, et al. Quality assurance of RapidArc in clinical practice using portal dosimetry. Br J Radiol. 2011; 84: 534–545 [PubMed: 21606069]

Fotina I, Hopfgartner J, Stock M, Steininger T, Lutgendorf-Caucig C, Georg D. Feasibility of CBCT-based dose calculation: comparative analysis of HU adjustment techniques. Radiother Oncol. 2012; 104:249–256. [PubMed: 22809588]

Fraass B, Doppke K, Hunt M, et al. American Association of Physicists in Medicine Radiation Therapy Committee Task Group 53: quality assurance for clinical radiotherapy treatment planning. Med Phys. 1998; 25:1773–1829. [PubMed: 9800687]

Francois P, Boissard P, Berger L, Mazal A. In vivo dose verification from back projection of a transit dose measurement on the central axis of photon beams. Phys Med. 2011; 27:1–10. [PubMed: 20615735]

Fredh A, Scherman JB, Fog LS, Munck af Rosenschöld P. Patient QA systems for rotational radiation therapy: a comparative experimental study with intentional errors. Med Phys. 2013; 40:031716. [PubMed: 23464311]

Fuangrod T, Woodruff HC, Van Uytven E, et al. A system for EPID-based real-time treatment delivery verification during dynamic IMRT treatment. Med Phys. 2013;40: 091907. [PubMed: 24007158]

Glendinning AG, Bonnett DE. Dosimetric properties of the Theraview fluoroscopic electronic portal imaging device. Br J Radiol. 2000; 73:517–530. [PubMed: 10884749]

Greer P, Fuangrod T, Woodruff H, Rowshanfarzad P, van Uytven E, McCurdy B. Real-time EPID-based dose verification system for detection of gross radiation treatment delivery errors. Int J Radiat Oncol Biol Phys. 2013;87: S120–S121.

Greer PB. Correction of pixel sensitivity variation and off-axis response for amorphous silicon EPID dosimetry. Med Phys. 2005; 32:3558–3568. [PubMed: 16475754]

Greer PB, Cadman P, Lee C, Bzdusek K. An energy-fluence convolution model for amorphous silicon EPID dose prediction. Med Phys. 2009; 36:547–555. [PubMed: 19291994]

Greer PB, Cadman P, Lee C, Bzdusek K. An energy fluence-convolution model for amorphous silicon EPID dose prediction. Med Phys. 2009; 36:547–555. [PubMed: 19291994]

Greer PB, Popescu CC. Dosimetric properties of an amorphous silicon electronic portal imaging device for verification of dynamic intensity modulated radiation therapy. Med Phys. 2003; 30:1618–1627. [PubMed: 12906179]

Greer PB, Vial P. Epid dosimetry. AIP Conf Proc. 2011:1345:129.

Greer PB, Vial P, Oliver L, Baldock C. Experimental investigation of the response of an amorphous silicon EPID to intensity modulated radiotherapy beams. Med Phys. 2007; 34:4389–4398. [PubMed: 18072504]

Glendinning AG and Bonnett DE. Dosimetric properties of the Theraview fluoroscopic electronic portal imaging device. Br J Radiol. 2000; 73: 517–530. [PubMed: 10884749]

Gustafsson H, Vial P, Kuncic Z, Baldock C, Denham JW, Greer PB. Direct dose to water dosimetry for pretreatment IMRT verification using a modified EPID. Med Phys. 2011; 38:6257–6264. [PubMed: 22047391]

Gustafsson H, Vial P, Kuncic Z, Baldock C, Greer PB. EPID dosimetry: effect of different layers of materials on absorbed dose response. Med Phys. 2009; 36:5665–5674. [PubMed: 20095279]

Hanson IM, Hansen VN, Olaciregui-Ruiz I, Van Herk M. Clinical implementation, and rapid commissioning of an EPID based in-vivo dosimetry system. Phys Med Biol. 2014;59: N171–N179. [PubMed: 25211121]

Heijmen BJ, Pasma KL, Kroonwijk M, et al. Portal dose measurement in radiotherapy using an electronic portal imaging device (EPID). Phys Med Biol. 1995; 40:1943–1955. [PubMed: 8587942]

Herman MG, Balter JM, Jaffray DA, et al. Clinical use of electronic portal imaging: Report of AAPM Radiation Therapy Committee Task Group 58. Med Phys. 2001; 28:712–737. [PubMed: 11393467]

Howell RM, Smith IPN, Jarrio CS. Establishing action levels for EPID-based QA for IMRT. J Appl Clin Med Phys. 2008; 9:16–25. [PubMed: 18716584]

Huq MS, Fraass BA, Dunscombe PB, et al. The report of Task Group 100 of the AAPM: application of risk analysis methods to radiation therapy quality management. Med Phys. 2016; 43:4209–4209. [PubMed: 27370140]

Hussein M, Adams EJ, Jordan TJ, Clark CH, Nisbet A. A critical evaluation of the PTW 2D-ARRAY seven29 and OCTAVIUS II phantom for IMRT and VMAT verification. J Appl Clin Med Phys. 2013;14(6):274–292.

Iori M, Cagni E, Paiusco M, Munro P, Nahum AE. Dosimetric verification of IMAT delivery with a conventional EPID system and a commercial portal dose image prediction tool. Med Phys. 2010; 37:377–390. [PubMed: 20175500]

Kausar A, Mani KR, Azhari HA, Zakaria GA. Patient-specific quality control for intensity-modulated radiation therapy and volumetric-modulated arc therapy using electronic portal imaging device and two-dimensional ion chamber array. J Radiother Pract. 2019; 18:26–31.

King BW, Clews L, Greer PB. Long-term two-dimensional pixel stability of EPIDs used for regular linear accelerator quality assurance. Australas Phys Eng Sci Med. 2011; 34:459–466. [PubMed: 22038292]

King BW, Greer PB. A method for removing arm backscatter from EPID images. Med Phys. 2013; 40:071703. [PubMed: 23822407]

Kirby MC, Glendinning AG. Developments in electronic portal imaging systems. Br J Radiol. 2006;79: S50–S65. [PubMed: 16980685]

Kirby MC, Williams PC. The use of an electronic portal imaging device for exit dosimetry and quality-control measurements. Int J Radiat Oncol Biol Phys. 1995; 31:593–603. [PubMed: 7852125]

Klein EE, Hanley J, Bayouth J, et al. Task Group 142 report: quality assurance of medical accelerators. Med Phys. 2009; 36:4197–4212. [PubMed: 19810494]

Ko L, Kim JO, Siebers JV. Investigation of the optimal backscatter for an aSi electronic portal imaging device. Phys Med Biol. 2004; 49:1723–1738. [PubMed: 15152927]

Koo M, Darko J, and Osei E. Retrospective analysis of portal dosimetry pre-treatment quality assurance of hybrid IMRT breast treatment plans. J of Radiother in Prac. 2021; 20 (1): 22–29.

Lam D, Zhang X, Li H, et al. Predicting gamma passing rates for portal dosimetry-based IMRT QA using machine learning. Med Phys. 2019; 46(10):4666–4675. [PubMed: 31386761]

Li W, Siebers JV, Moore JA. Using fluence separation to account for energy spectra dependence in computing dosimetric a-Si EPID images for IMRT fields. Med Phys. 2006; 33:4468–4480. [PubMed: 17278798]

Lim SB, Tsai CJ, Yu Y, et al. Investigation of a novel decision support metric for head and neck adaptive radiation therapy using a real-time in vivo portal dosimetry system. Technol Cancer Res Treat. 2019; 18:1–6.

Liu B, Adamson J, Rodrigues A, Zhou F, Yin FF, Wu Q. A novel technique for VMAT QA with EPID in cine mode on a Varian TrueBeam linac. Phys Med Biol. 2013; 58:6683–6700. [PubMed: 24018655]

Louwe RJW, McDermott LN, Sonke JJ, et al. The long-term stability of amorphous silicon flat panel imaging devices for dosimetry purposes. Med Phys. 2004; 31:2989–2995. [PubMed: 15587651]

Luchka K, Chen D, Shalev S, Gluhchev G, Rajapakshe R. Assessing radiation and light field congruence with a video based electronic portal imaging device. Med Phys. 1996; 23:1245–1252. [PubMed: 8839420]

Mans A, Remeijer P, Olaciregui-Ruiz I, et al. 3D Dosimetric verification of volumetric-modulated arc therapy by portal dosimetry. Radiother Oncol. 2010; 94:181–187. [PubMed: 20089323]

Masi L, Casamassima F, Doro R, Francescon P. Quality assurance of volumetric modulated arc therapy: evaluation and comparison of different dosimetric systems. Med Phys. 2011; 38:612–621. [PubMed: 21452698]

McCurdy BM, Luchka K, Pistorius S. Dosimetric investigation and portal dose image prediction using an amorphous silicon electronic portal imaging device. Med Phys. 2001; 28:911–924. [PubMed: 11439488]

McCurdy BMC, Greer PB. Dosimetric properties of an EPID for real-time dose verification. Med Phys. 2009; 36:4303–4303.

McCurdy BMC, Luchka K, Pistorius S. Dosimetric investigation and portal dose image prediction using an amorphous silicon electronic portal imaging device. Med Phys. 2001; 28:911–924. [PubMed: 11439488]

McCurdy BMC, McCowan PM. In vivo dosimetry for lung radiotherapy including SBRT. Phys Med. 2017; 44:123–130. [PubMed: 28576581]

McCurdy BMC, Greer PB, Bedford J Electronic portal imaging device (EPID) dosimetry. In: Mijnheer B, ed. Clinical 3D Dosimetry in Modern Radiation Therapy. Boca Raton, FL: CRC Press; 2017:171–201.

McDermott LN, Louwe RJ, Sonke JJ, van Herk MB, Mijnheer BJ. Dose-response and ghosting effects of an amorphous silicon electronic portal imaging device. Med Phys. 2004; 31:285–295. [PubMed: 15000614]

McDermott LN, Nijsten SM, Sonke JJ, Partridge M, van Herk M, Mijnheer BJ. Comparison of ghosting effects for three commercial a-Si EPIDs. Med Phys. 2006; 33:2448–2451. [PubMed: 16898447]

McDermott LN, Wendling M, Asselen B, et al. Clinical experience with EPID dosimetry for prostate IMRT pre-treatment dose verification. Med Phys. 2006; 33:3921–3930. [PubMed: 17089854]

Meertens H, van Herk M, Weeda J. A liquid ionization detector for digital radiography of therapeutic megavoltage photon beams. Phys Med Biol. 1985; 30:313–321. [PubMed: 3923505]

Miften M, Olch A, Mihailidis D, et al. Tolerance limits and methodologies for IMRT measurement-based verification QA: recommendations of AAPM Task Group No. 218. Med Phys. 2018;45: e53–e83. [PubMed: 29443390]

Mijnheer B. Clinical 3D dosimetry in modern radiation therapy. In: Mijnheer B, ed. Boca Raton, FL: CRC Press; 2017 a:461–490.

Mijnheer B EPID-based dosimetry and its relation to other 2D and 3D dose measurement techniques in radiation therapy. J Phys: Conf Ser. 2017b; 847:012024.

Mijnheer B, Jomehzadeh A, Gonzalez P, et al. Error detection during VMAT delivery using EPID-based 3D transit dosimetry. Phys Med. 2018; 54:137–145. [PubMed: 30337003]

Mijnheer B, Olaciregui-Ruiz I, Rozendaal R, et al. 3D EPID-based in vivo dosimetry for IMRT and VMAT. J Phys: Conf Ser. 2013; 444:012011.

Mijnheer BJ, González P, Olaciregui-Ruiz I, Rozendaal RA, van Herk M, Mans A. Overview of 3-year experience with large-scale electronic portal imaging device-based 3-dimensional transit dosimetry. Pract Radiat Oncol. 2015;5: e679–e687. [PubMed: 26421834]

Miri N, Keller P, Zwan BJ, Greer P. EPID-based dosimetry to verify IMRT planar dose distribution for the aS1200 EPID and FFF beams. J Appl Clin Med Phys. 2016;17(6):292–304. [PubMed: 27929502]

Miri N, Lehmann J, Legge K, Vial P, Greer PB. Virtual EPID standard phantom audit (VESPA) for remote IMRT and VMAT credentialing. Phys Med Biol. 2017; 62:4293–4299. [PubMed: 28248642]

Moran JM, Roberts DA, Nurshev TS, Antonuk LE, El-Mohri Y, Fraass BA. An active matrix flat panel dosimeter (AMFPD) for in-phantom dosimetric measurements. Med Phys. 2005; 32:466–472. [PubMed: 15789593]

Nailon WH, Welsh D, McDonald K, et al. EPID-based in vivo dosimetry using Dosimetry Check: overview and clinical experience in a 5-yr study including breast, lung, prostate, and head and neck cancer patients. J Appl Clin Med Phys. 2019;20(1):6–16.

Nelms BE, Opp D, Robinson J, et al. VMAT QA: measurement-guided 4D dose reconstruction on a patient. Med Phys. 2012; 39:4228–4238. [PubMed: 22830756]

Nicolini G, Clivio A, Vanetti E, et al. Evaluation of an aSi-EPID with flattening filter free beams: applicability to the GLAaS algorithm for portal dosimetry and first experience for pretreatment QA of RapidArc. Med Phys. 2013;40: 111719. [PubMed: 24320427]

Nicolini G, Fogliata A, Vanetti E, Clivio A, Cozzi L. GLAaS: an absolute dose calibration algorithm for an amorphous silicon portal imager. Applications to IMRT verifications. Med Phys. 2006; 33:2839–2851. [PubMed: 16964860]

Nijsten SM, Minken AW, Lambin P, Bruinvis IA. Verification of treatment parameter transfer by means of electronic portal dosimetry. Med Phys. 2004; 31:341–347. [PubMed: 15000620]

Nijsten SMJJG, Van Elmpt WJC, Jacobs M, et al. A global calibration model for a-Si EPIDs used for transit dosimetry. Med Phys. 2007; 34:3872–3884. [PubMed: 17985633]

Nyflot M, Thammasorn P, Wootton LS, et al. Deep learning for patient-specific quality assurance: Identifying errors in radiotherapy delivery by radiomic analysis of gamma images with convolutional neural networks. Med Phys. 2018; 46(2):456–464. [PubMed: 30548601]

Olaciregui-Ruiz I, Beddar S, Greer P, et al. In vivo dosimetry in external beam photon radiotherapy: requirements and future directions for research, development, and clinical practice. Phys Imaging Radiat Oncol. 2020; 15:108–116. [PubMed: 33458335]

Olaciregui-Ruiz I, Rozendaal R, van Oers RFM, Mijnheer B, Mans A. Virtual patient 3D dose reconstruction using in air EPID measurements and a back-projection algorithm for IMRT and VMAT treatments. Phys Med. 2017; 37:49–57. [PubMed: 28535915]

Olaciregui-Ruiz I, Vivas-Maiques B, Kaas J, et al. Transit and non-transit 3D EPID dosimetry versus detector arrays for patient specific QA. J Appl Clin Med Phys. 2019;20(6):79–90. [PubMed: 31083776]

Olch AJ, O'Meara K, Wong KK. First report of the clinical use of a commercial automated system for daily patient QA using EPID exit images. Adv Radiat Oncol. 2019; 4:722–728. [PubMed: 31681865]

Pardo E, Novais JC, Lopez MYM, Maqueda SR. On flattening filter-free portal dosimetry. J Appl Clin Med Phys. 2016;17(4):132–145.

Parent L, Fielding AL, Dance DR, Seco J, Evans PM. Amorphous silicon EPID calibration for dosimetric applications: comparison of a method based on Monte Carlo prediction of response with existing techniques. Phys Med Biol. 2007; 52:3351–3368. [PubMed: 17664548]

Parent L, Seco J, Evans PM, Fielding A, Dance DR. Monte Carlo modelling of a-Si EPID response: the effect of spectral variations with field size and position. Med Phys. 2006; 32:4527–4540.

Passarge M, Fix MK, Manser P, Stampanoni MF, Siebers JV. A Swiss cheese error detection method for real-time EPID-based quality assurance and error prevention. Med Phys. 2017; 44:1212–1223. [PubMed: 28134989]

Persoon LC, Podesta M, Nijsten SM, Troost EG, Verhaegen F. Time-resolved versus integrated transit planar dosimetry for volumetric modulated arc therapy: patient-specific dose differences during treatment, a proof of principle. Technol Cancer Res Treat. 2016;15:NP79–NP87. [PubMed: 26655145]

Piermattei A, Greco F, Azario L, et al. A national project for in vivo dosimetry procedures in radiotherapy: first results. Nucl Instrum Methods Phys Res B. 2012; 274:42–50.

Piermattei A, Cilla S, Grimaldi L, et al. Integration between in vivo dosimetry and image guided radiotherapy for lung tumors. Med Phys. 2009; 36:2206–2214. [PubMed: 19610309]

Piermattei A, Greco F, Grusio M, et al. A validation study of a dedicated software for an automated in vivo dosimetry control in radiotherapy. Med Biol Eng Comput. 2018; 56: 1939–1947. [PubMed: 29682674]

Podesta M, Nijsten SM, Snaith J, et al. Measured vs simulated portal images for low MU fields on three accelerator types: possible consequences for 2D portal dosimetry. Med Phys. 2012; 39:7470–7479. [PubMed: 23231296]

Podesta M, Nijsten SMJJG, Persoon LCGG, Scheib SG, Baltes C, Verhaegen F. Time dependent pre-treatment EPID dosimetry for standard and FFF VMAT. Phys Med Biol. 2014; 59:4749–4768. [PubMed: 25088064]

Renner WD, Norton K, Holmes T. A method for deconvolution of integrated electronic portal images to obtain incident fluence for dose reconstruction. J Appl Clin Med Phys. 2005;6(4):22–39.

Ricketts K, Navarro C, Lane K, et al. Clinical experience, and evaluation of patient treatment verification with a transit dosimeter. Int J Radiat Oncol Biol Phys. 2016; 95:1513–1519. [PubMed: 27262359]

Ricketts K, Navarro C, Lane K, et al. Implementation and evaluation of a transit dosimetry system for treatment verification. Phys Med. 2016; 32:671–680. [PubMed: 27134042]

Rowshanfarzad P, McCurdy BMC, Sabet M, Lee C, O'Connor DJ, Greer PB. Measurement and modelling of the effect of support arm backscatter on dosimetry with a Varian EPID. Med Phys. 2010; 37:2269–2278. [PubMed: 20527561]

Rowshanfarzad P, McGarry CK, Barnes MP, Sabet M, Ebert MA. An EPID-based method for comprehensive verification of gantry, EPID and the MLC carriage positional accuracy in Varian linacs during arc treatments. Radiat Oncol. 2014; 9:249. [PubMed: 25424471]

Rozendaal RA, Mijnheer BJ, Hamming-Vrieze O, Mans A, van Herk M. Impact of daily anatomical changes on EPID-based in vivo dosimetry of VMAT treatments of head-and-neck cancer. Radiother oncol. 2015; 116:70–74. [PubMed: 26142267]

Schroder L, Stankovic U, Sonke JJ. Technical Note: Long-term stability of Hounfield unit calibration for cone beam computed tomography. Med Phys. 2020; 47(4):1640–1644. [PubMed: 31923327]

Siebers JV, Kim JO, Ko L, Keall PJ, Mohan R. Monte Carlo computation of dosimetric amorphous silicon electronic portal images. Med Phys. 2004; 31:2135–2146. [PubMed: 15305468]

Smilowitz JB, Das IJ, Feygelman V, et al. AAPM Medical Physics Practice Guideline 5.a.: commissioning and QA of treatment planning dose calculations—megavoltage photon and electron beams. J Appl Clin Med Phys. 2016; 16(5):14–34.

Son J, Baek T, Lee B, et al. A comparison of the quality assurance of four dosimetric tools for intensity modulated radiation therapy. Radiol Oncol. 2015; 49:307–313. [PubMed: 26401138]

Spreeuw H, Rozendaal R, Olaciregui-Ruiz I, et al. Online 3D EPID-based dose verification: proof of concept. Med Phys. 2016; 43:3969–3974. [PubMed: 27370115]

Sterckx B, Steinseifer I and Wendling M. In vivo dosimetry with an electronic portal imaging device for prostate cancer radiotherapy with an endorectal balloon. Phys Imaging Radiat Oncol. 2019; 12: 7–9. [PubMed: 33458288]

Valdes G, Chan MF, Lim SB, Scheuermann R, Deasy JO, Soldberg TD. IMRT QA using maching learning: A multi-institutional validation. J Appl Clin Med Phys. 2017; 18(5): 279–284. [PubMed: 28815994]

van Elmpt W, McDermott L, Nijsten S, Wendling M, Lambin P, Mijnheer B. A literature review of electronic portal imaging for radiotherapy dosimetry. Radiother Oncol. 2008; 88:289–309. [PubMed: 18706727]

Van Esch A, Depuydt T, Huyskens DP. The use of an aSi-based EPID for routine absolute dosimetric pre-treatment verification of dynamic IMRT fields. Radiother Oncol. 2004; 71:223–234. [PubMed: 15110457]

Van Esch A, Huyskens DP, Hirschi L, Baltes C. Optimized Varian aSi portal dosimetry: development of datasets for collective use. J Appl clin med phys. 2013; 14(6):82–99.

Van Zijtveld MV, Dirkx ML, de Boer HCJ, Heijmen BJ. Dosimetric pre-treatment verification of IMRT using an EPID; clinical experience. Radiother Oncol. 2006; 81:168–175. [PubMed: 17055604]

Vieillevigne L, Molinier J, Brun T, Ferrand R. Gamma index comparison of three VMAT QA systems and evaluation of their sensitivity to delivery errors. Phys Med. 2015; 31:720–725. [PubMed: 26095758]

Vinall AJ, Williams AJ, Currie VE, Van Esch A, Huyskens D. Practical guidelines for routine intensity-modulated radiotherapy verification: pre-treatment verification with portal dosimetry and treatment verification with in vivo dosimetry. Br J Radiol. 2010; 83:949–957. [PubMed: 20965905]

Wang S, Gardner JK, Gordon JJ, et al. Monte Carlo-based adaptive EPID dose kernel accounting for different field size responses of imagers. Med Phys. 2009; 36:3582–3595. [PubMed: 19746793]

Wang X, Chen L, Xie C, et al. Experimental verification of a 3D in vivo dose monitoring system based on EPID. Oncotarget 2017; 8:109619–109631. [PubMed: 29312634]

Warkentin B, Steciw S, Rathee S, Fallone BG. Dosimetric IMRT verification with a flat-panel EPID. Med Phys. 2003; 30:3143–3155. [PubMed: 14713081]

Wendling M, McDermott LN, Mans A, et al. In aqua vivo EPID dosimetry. Med Phys. 2012; 39:367–377. [PubMed: 22225306]

Wendling M, McDermott LN, Mans A, Sonke JJ, van Herk M, Mijnheer BJ. A simple backprojection algorithm for 3D in vivo EPID dosimetry of IMRT treatments. Med Phys. 2009; 36:3310–3321. [PubMed: 19673227]

Wexler A, Gu B, Goddu S, Mutic M, Yaddanapudi S, Olsen L, Harry T, Noel C, Pawlicki T, Mutic S and Cai B. FMEA of manual and automated methods for commissioning a radiotherapy treatment planning system. Med Phys.2017; 44: 4415–4425. [PubMed: 28419482]

Wolfs CJA, Canters RAM, Verhaegen F. Identification of treatment error types for lung cancer patients using convolutional neural networks and EPID dosimetry. Radiother Oncol. 2020; 153:243–249. [PubMed: 33011206]

Woodruff HC, Fuangrod T, Van Uytven E, et al. First experience with real-time EPID-based delivery verification during IMRT and VMAT sessions. Int J Radiat Oncol Biol Phys. 2015; 93:516–522. [PubMed: 26460993]

Wu C, Hosier KE, Beck KE, et al. On using 3D gamma-analysis for IMRT and VMAT pretreatment plan QA. Med Phys. 2012; 39:3051–3059. [PubMed: 22755690]

Yedekci Y, Biltekin F, Ozyigit G. Feasibility study of an electronic portal imaging based in vivo dose verification system for prostate stereotactic body radiotherapy. Phys Med. 2019; 64:204–209. [PubMed: 31515021]

Zhang J, Cheng Z, Fan Z, Zhang Q, Zhang X, Yang R, and Wen J. A feasibility study for in vivo treatment verification of IMRT using Monte Carlo dose calculation and deep learning-based modelling of EPID detector response. Radiat Oncol. 2022; 17:31:1–12. [PubMed: 34980178]

Zhuang AH, Olch AJ. Sensitivity study of an automated system for daily patient QA using EPID exit dose images. J Appl Clin Med Phys. 2018; 19(3):114–124.

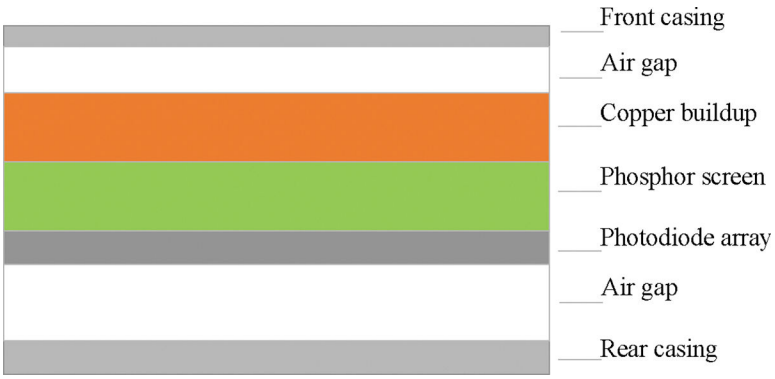

Figure 1.
Main components of an a-Si EPID.

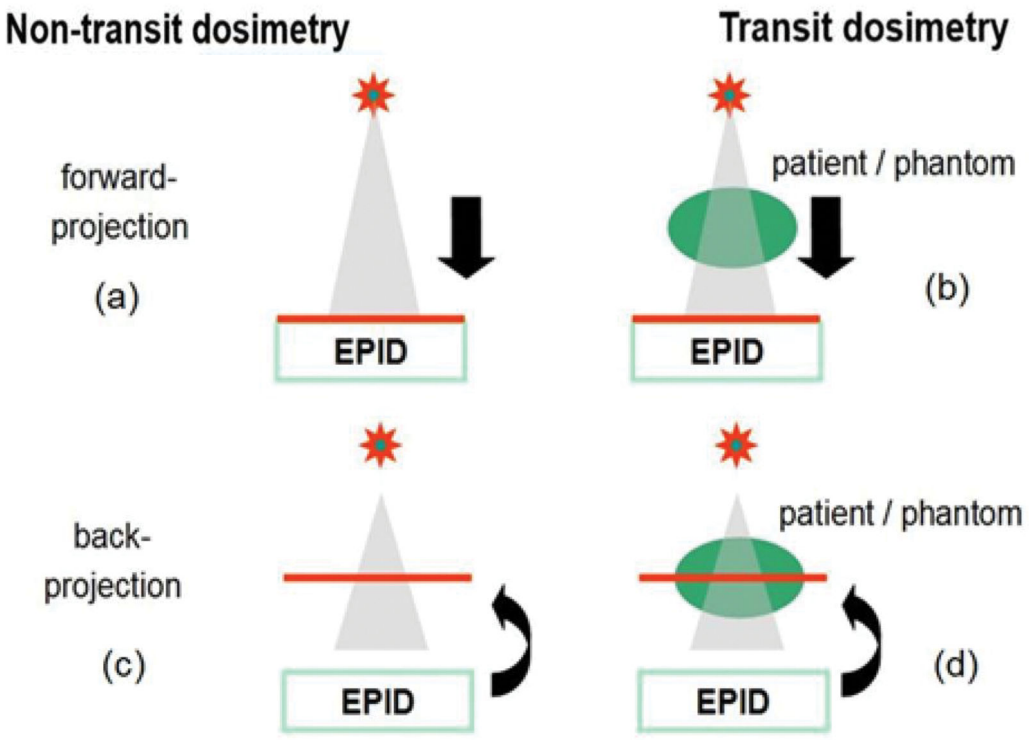

Figure 2.
Schematic representation of the various EPID-based PSQA techniques. (a) and (b) Forward methods compare measured 2D images or dose distributions with predicted images or dose distributions at the EPID level. Back-projection methods, both (c) non-transit and (d) transit, provide dose distributions in a phantom or patient. (Reproduced from Mijnheer 2017[b]).

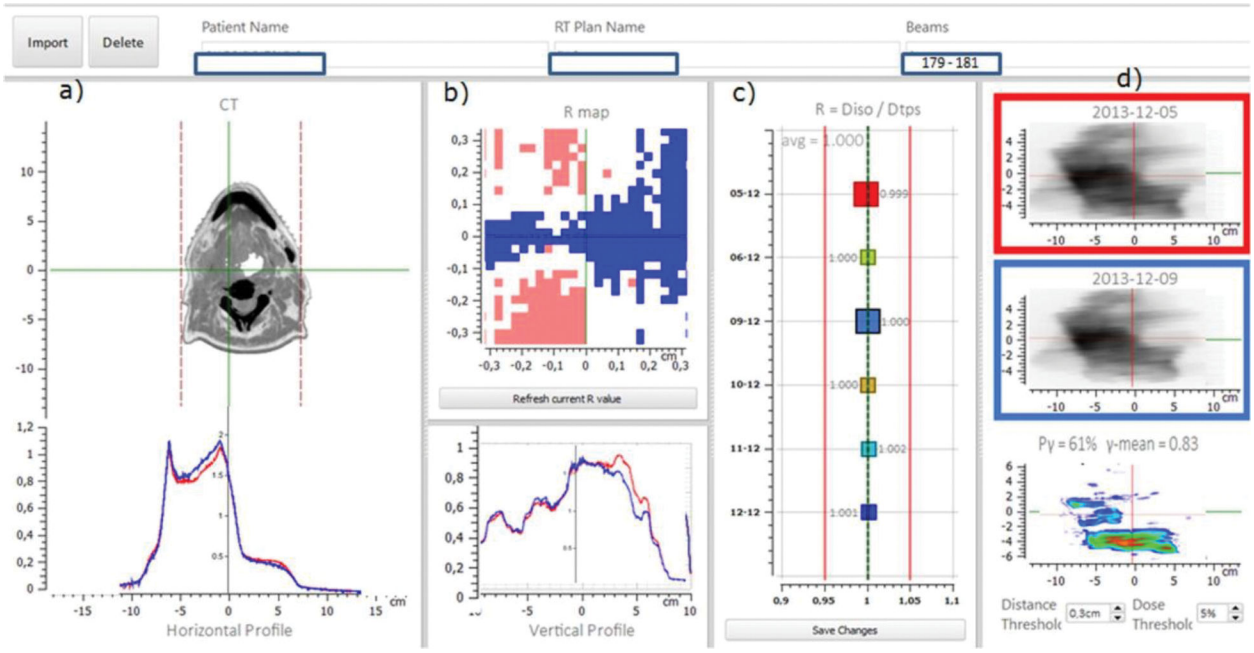

Figure 3.

Computer screen showing the SOFTDISO interface for IVD results. The screen is subdivided into four areas. From the left: (a) patient CT slice at isocenter level and the in-plane EPID profiles of two measurements; (b) the pixel area around the beam central axis consisting of 9 × 9 pixels (corresponding roughly to the TPS grid) and the cross-plane EPID profiles; (c) the results for *R* ratios, the ratios between the measured dose, and the dose calculated by the TPS in the pixel area around the beam central axis, obtained at different days; and (d) the daily EPID-integrated images obtained at two different days and their γ analysis. The red and blue data in the four figures have been obtained on two different days: December 5 and December 9, 2013, respectively. (Reproduced from Cilla, Meluccio et al. 2016).

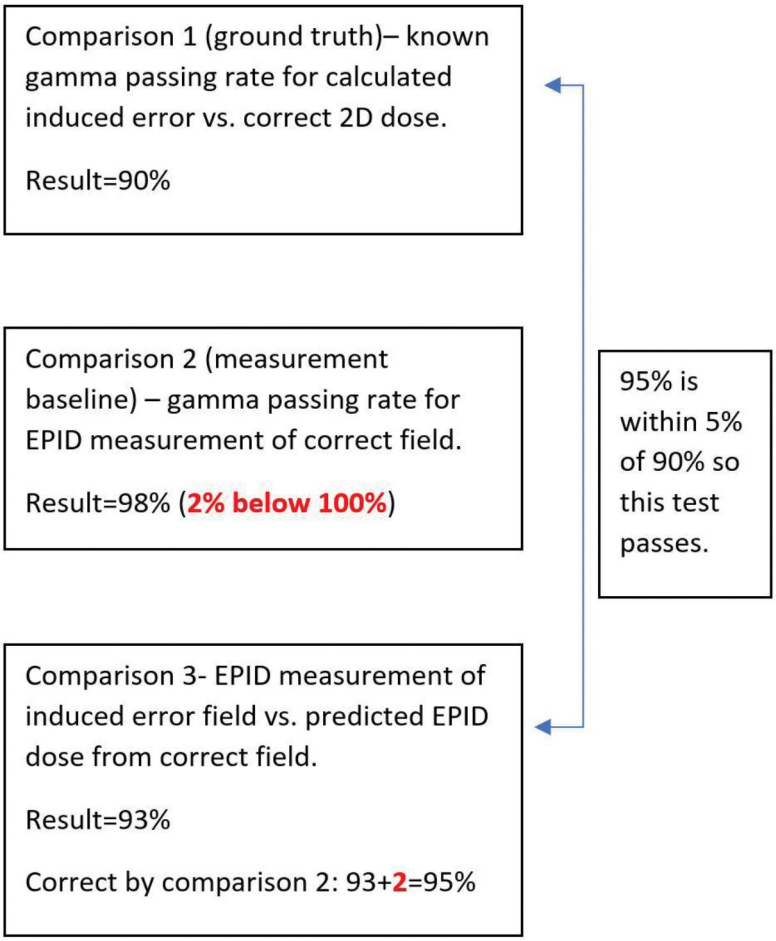

Figure 4.
Steps involved in verification of the predicted dose.

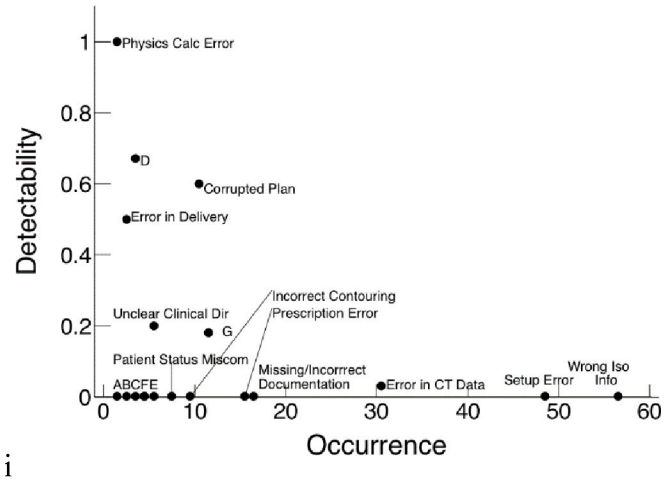

i

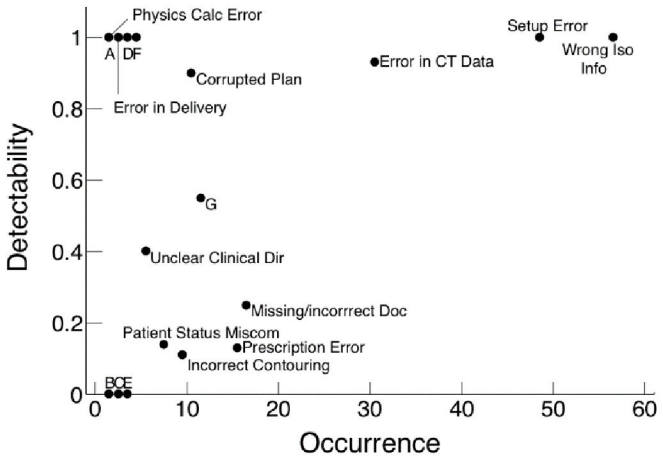

(a) (b)

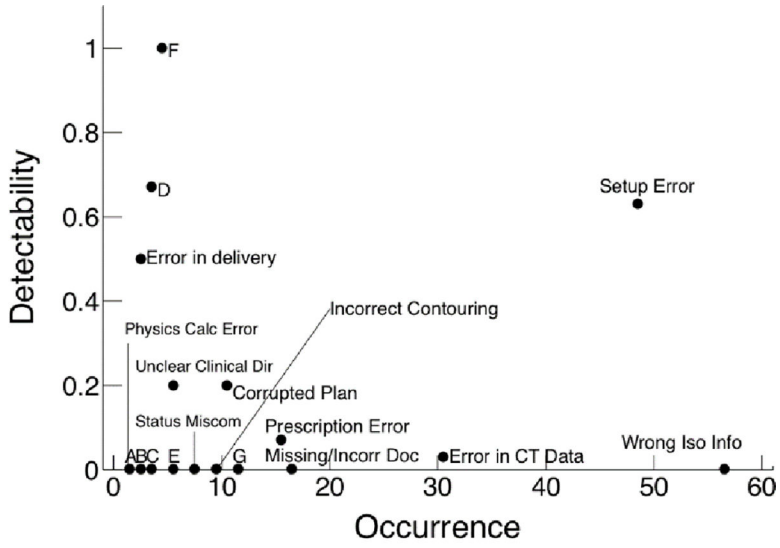

(c)

Figure 5.

Graphical representation of the ability of EPID QA to detect failure modes for (a) pretreatment, (b) first fraction transit, and (c) all fraction transit dosimetry as reported by Bojechko et al (Bojechko, Phillips et al. 2015). Each graph contains points representing a specific failure mode from the radiotherapy process scored for probability of occurrence and detectability. For example, pretreatment EPID dosimetry has high detectability for errors such as physics calculation error or treatment machine error, but low detectability for a number of failure modes such as wrong isocenter info, wrong or faulty equipment used, or movement on table. Comparisons between graphs demonstrate the potential advantages of specific EPID QA implementation; for instance, first fraction transit dosimetry has higher detectability of many failure modes, including a cluster of high occurrence failure modes such as wrong isocenter info, setup error, and error in CT data, while the detectability of these modes is lower for pretreatment and all fraction transit dosimetry. Legend for abbreviated failure modes: A: wrong or faulty equipment used, B: record and verify system down, C: personnel could not be contacted, D: treatment machine error, E: scheduling error, F: movement on table, and G: error in field planning.

Table 1.

Summary of current EPID technology and dosimetry products.

Software	Version	Compatible linac	Characteristics		Comparison calculation	Reference (Derived from EPID Images)
Portal Dosimetry (Varian)	1.7	Varian	Pre-treatment	2D	vendor algorithm	Image
Adaptivo (Standard Imaging)	1.5	Varian	Pre-treatment	2D	vendor algorithm	Image
		Varian	Transit	2D	vendor algorithm	Image
SOFTDISO (Best Medical)	1.0	Varian Elekta	Pre-treatment	2D	vendor algorithm	Image (non dosimetric)
		Varian Elekta	Transit	0D	TPS	Dose in patient (at isocenter)
Epiqa (EPIdos)	5.0	Varian Elekta	Pre-treatment	2D	TPS	Dose in water slab
EPIbeam and EpiGray (DOSIsoft)	1.0.6 and 2.0.10	Varian Elekta	Pre-treatment	2D	vendor algorithm	Dose in water slab
		Varian Elekta	Transit	0D	TPS	Dose in patient
EPIDose (Sun Nuclear)	8.4 (SNC Patient)	Varian Elekta	Pre-treatment	2D	TPS	Dose in water slab
PerFRACTION SunCHECK Patient (Sun Nuclear)	2.11.0	Varian Elekta	Pre-treatment	2D	vendor algorithm	Dose in water slab
		Varian Elekta	Pre-treatment	3D	TPS	Dose in patient (non dosimetric)
		Varian Elekta	Transit	2D	vendor algorithm	Dose in water slab
		Varian Elekta	Transit	3D	TPS	Dose in patient (non dosimetric)
RadCalc EPID (LAP)	7.2	Varian Elekta	Pre-treatment	3D	TPS	Dose in patient
		Varian Elekta	Transit	3D	TPS	Dose in patient
3DVH (Sun Nuclear)	3.3	Varian Elekta	Pre-treatment	3D	TPS	Dose in patient
iViewDose (Elekta)	1.0.1	Elekta	Transit	3D	TPS	Dose in patient

Table 2.

Characteristics of the currently available EPID systems.

	Varian aS1000 (C-Series and Truebeam)*	Varian aS1200 (Truebeam)	Varian aS1200 (Halcyon/Ethos)	Elekta iViewGT™ (AL panel)	Elekta iViewGT (AP panel)	Elekta Unity (AP panel)†
Moveable lateral, sup-inf	Yes	Yes	No	Yes	Yes	No
Moveable up-down	Yes	Yes	No	No	No	No
SID (cm)	100–180	100–180	154	160	160	265.3
Dimensions (cm^2) lateral × superior-inferior	40 × 30	43 × 43 (40 × 40) dosimetry mode	43 × 43	41 × 41	41 × 41	41 × 41
Dimensions at isocenter (cm^2)	40 × 30	43 × 43	27.9 × 27.9	25.6 × 25.6	25.6 × 25.6	22.3 × 22.3‡
Pixel size (mm^2)	0.392 × 0.392	0.336 × 0.336	0.336 × 0.336	0.400 × 0.400	0.400 × 0.400	0.400 × 0.400
Frame rate (Hz)	Up to 20§	Up to 20	Up to 20	3	Up to 15	Up to 15
DICOM image format export (including DPS)	Yes#	Yes	Yes	**	**	**
Other dosimetric format				Image data in HIS or lossless JPEG format Gantry/DPS info in text XML file (license required)††	Image data in HIS or lossless JPEG format Gantry/DPS info in text XML file (license required)††	Image data in HIS or lossless JPEG format Gantry/DPS info in text XML file (license required)††
Dosimetric cine mode acquisition (including DPS)	Yes C-Series‡‡ No Truebeam	No§§	No§§	Yes††¶¶##	Yes††¶¶##	Yes††¶¶##
Support for FFF imaging	Yes***	Yes	Yes	No	Yes	Yes

*Varian aS500-II is the same panel as an aS1000 except with resolution set to 0.784 × 0.784 mm^2.

†The acquisition software is called MVIC which is a new software based on iViewGT.

‡Source-isocenter distance = 143.5 cm. Unattenuated region free of gradient coils ~10 × 22 cm^2 at isocenter.

§On C-Series up to 23 frames per second.

¶DPS (required factor to scale stored pixel values to integrated signal).

#Mosaiq does not retain DPS.

**Auto-Push of DICOM images works in iViewGT only for integrated images. The movie exposure images do not DICOM Auto-Push. If you manually export a Movie, iViewGT only sends the first frame. For EPID dosimetry, the data are accessed by pulling the data from the iViewGT database rather than pushing via DICOM.

[††] Assumes iViewGT version ≥3.4.1. With older panels, typically also versions of iViewGT (<3.4.1) are installed. There is no support for cine mode with this (neither gantry nor DPS information per frame is available, and there is a maximum of 255 frames per acquisition).

[‡‡] Frames at start and end of irradiation discarded reducing dosimetric accuracy, limit of number of frames.

[§§] Cumulative DICOM frames can be exported using IPS. Each frame is a sum of all frames to that point. The limit of frames per acquisition can be exported. Requires external software to unpack individual frames.

[¶¶] Individual JPEG frames files saved to patient folder. XML file with frame information including DPS and gantry angle (dosimetry license required).

[##] iViewGT displayed images always have DPS applied. When DPS is not licensed, the pixel factor is encoded when written to the _Frame.xml file as a negative value so that it can be distinguished from an unencoded pixel factor which is always positive.

[***] Only for Truebeam systems with software version 2.0 or higher with minimum SID = 125 cm for 6XFFF (1400 MU/min) and SID = 165 cm for 10XFFF (2400 MU/min).

Table 3.

Review of studies on sensitivity and specificity of each EPID-based PSQA system to detect errors.

System	Author	Tests performed	Results
Portal Dosimetry Epidose	Bailey et al. 2012	1 patient plan, global dose TPS beam model commissioning error	Portal Dosimetry not sensitive to 5% MU/cGy error while Epidose was sensitive
Dosimetry Check (RadCalc EPID)	Wu et al. 2012	10 patient plans with MLC and gantry offset errors	PTV result sensitive to MLC, V10% sensitive to gantry
Epiqa	Fredh et al. 2013	4 patient plans with introduced MU, MLC, and collimator errors	100% detected by Epiqa, better than other detectors (Delta4, Octavius, Compass)
Epiqa	Vieillevigne et al. 2015	4 patient plans with introduced MLC, collimator, gantry, couch errors	Performance similar to other detectors (ArcCheck, PTW 794)
PerFRACTION Portal Dosimetry	Bresciani et al. 2018	1 patient plan with introduced MU, MLC errors	3D (log file based) method compared to Portal Dosimetry. Similar sensitivity, higher specificity

Table 4.

A summary of clinical studies for pretreatment EPID based PSQA.

System	Author	Tests performed	Results
Dosimetry Check (RadCalc EPID)	Chendi et al. 2021	20 FFF plans, compared to Octavius phantom measurement and TPS calculation (in-patient CT)	Poor correlation in gamma-pass rates
Epiqa	Fogliata et al. 2011	295 patient VMAT plans, 5 centers	Mean gamma 97.1±2.4% at 3%,3mm
Epiqa	Nicolini et al. 2013	74 arcs VMAT FFF	Similar to non FFF if > 150 cm EPID distance
Portal Dosimetry	Howell et al. 2008	152 patient IMRT plans (1152 fields)	Mean gamma value tolerances established
Portal Dosimetry	Iori et al. 2010	23 arcs VMAT	Same results as IMRT but using external EPID fixation device
Portal Dosimetry	Bailey et al. 2012	Prostate, head neck, breast IMRT (126 fields)	Off axis breast tangents lower results, may not adequately model off axis
Portal Dosimetry	Ballangrud et al. 2018	40 multitarget SRS deliveries	γ pass rate of greater than 95% for most fields at 3%/2 mm criteria with a 10% threshold
Portal Dosimetry	Covington et al. 2019	36 plans single-target SRS VMAT QA for at 10FFF energy	composite EPID image of the two arcs 3%/2 mm criteria with 10% threshold a 100% pass rate
Portal Dosimetry	Koo et al. 2020	200 breast IMRT plans	Average gamma passing rate of 98·4 ± 4·3 for 2%/2 mm symmetric plans and 89·7 ± 9·5 for 2%/2 mm asymmetric plans

Table 5.

Errors found using commercially available EPID-based transit dosimetry systems (adapted from Mijnheer 2017[b]).

Potential error	Error type	References
Machine-related	Transfer error	Mans et al., 2010; Mijnheer et al., 2015
Plan-related	Dose calculation error	Mans et al., 2010; Fidanzio et al., 2015; Mijnheer et al., 2015; Bossuyt et al., 2020
	Immobilization system not included in the treatment plan	Fidanzio et al., 2015
	Bolus material not taken into account	Mijnheer et al., 2015
Patient-related: anatomy changes	Changes in atelectasis, pleural effusion, and development of pneumonia	Piermattei et al., 2009; Mans et al., 2010; Wendling et al., 2012; Fidanzio et al., 2015; Mijnheer et al, 2015; Bossuyt et al., 2020
	Variation in patient contour due to tumor reduction or growth, or when the patient becomes more relaxed during treatment	Mans et al., 2010; Fidanzio et al., 2014; Olch et al., 2019; Bossuyt et al., 2020
	Gas pockets in the reference dose distribution resulting in an under-dose in the PTV during treatment	Cilla et al., 2014; Fidanzio et al., 2015; Olch et al., 2019; Bossuyt et al., 2020
	Weight loss resulting in an over-dose in the PTV during treatment	Mans et al., 2010; Cilla et al., 2014, 2016; Olch et al., 2019
	Incomplete bladder filling resulting in an over-dose in the PTV during treatment	Ricketts et al., 2016
Patient-related: delivery errors	Bar of the treatment couch in the entrance beam during treatment	Piermattei et al., 2009; Fidanzio et al., 2015; Bossuyt et al., 2020
	Imperfect immobilization allowing the patient to move during treatment	Hanson et al., 2014; Cilla et al., 2016
	Wrong patient setup during treatment	Fidanzio et al., 2015; Mijnheer et al., 2015; Olch et al., 2019; Bossuyt et al., 2020
	Wrong position of belly board	Bossuyt et al., 2020
	Misalignment of the beams: Variation in breast contour: lateral breast treatments at their center generally resulted in better dosimetric conformance than supine treatments	Celi, Costa et al. 2016

Table 6.

Recommended tests to ensure the EPID will function accurately as a dosimeter.

Test	Description	Tolerance
EPID positioning	Determine the reproducibility of EPID positioning at gantry zero by three EPID deployments with a 10 × 10 cm^2 field acquired after each deployment. Establish the center of each field in X and Y directions and measure the distance to the center of the panel for all three acquisitions to determine reproducibility.	Vendor specification or ≤2 mm
EPID positioning with gantry rotation	Repeat the 10 × 10 cm^2 image at 45° gantry angle increments. Measure the center of each field in X and Y. Measure the difference relative to gantry zero position. Convert to mm using the known pixel dimension.	Vendor specification or ≤2 mm
Linearity with dose	First determine that the Linac MU linearity is within TG 142 tolerance, then irradiate a 10 × 10 cm^2 field with varying MU settings from 2 to 500. Measure the integrated pixel value (IPV) at the center of each field. Determine the IPV per MU relative to 100 MU. *	Vendor specification or within 2% (5% for MU < 5)
Uniformity	After flood-field calibration, irradiate the entire EPID sensitive area with 100MU at the same SID. Measure the mean and SD of the pixel values within a large region that excludes the detector edges and penumbra (2 cm inside the panel edges and 0.5 cm inside field edges). Calculate the SD as a percentage of the mean.	Uniformity following panel calibration ±2% (SD as a percentage of the mean)
Reproducibility	EPID reproducibility is important and needs to be stable over months and this should be confirmed over the first months following installation. The EPID response reproducibility at the center of the 10 × 10 cm^2 field needs to be sampled weekly for at least 1 mo period and be stable (adjusted for linac output). The frequency of EPID dose response recalibrations should be tracked over time to ensure EPID panel has consistent performance.	Dosimetric reproducibility of ±2%

* Gamma analyses may have failures in situations when a small number of MUs is delivered if both Linac MU linearity and EPID linearity are off in the same direction.

Table 7.

Monthly routine QA for EPID-based QA systems

2D PTQA			
Test	**Technique**	**Metric**	**Tolerance**
Dose constancy	10 × 10cm static field	% Dose difference *	±2%
2D static field	25 × 25cm static field	2D γ	Baseline ± 2% †
Patient/test plan	IMRT	2D γ	Baseline ± 2% †
Patient/test plan	VMAT	2D γ	Baseline ± 2% †
Positioning	25 × 25cm static field	Distance	±2 mm (non-SBRT/SRS)
	@ Cardinal angles		±1 mm (SBRT/SRS)
Scaling	25 × 25cm static field	Distance	±2 mm
2D Transit Dosimetry QA			
Test	**Technique**	**Comparison Method**	**Tolerance**
Dose constancy	25 × 25cm	% Dose difference	±2%
2D static field	25 × 25cm	2D γ	Baseline ± 3% †
Patient/test plan	IMRT	2D γ	Baseline ± 3% †
Patient/test plan	VMAT	2D γ	Baseline ± 3% †

* Mean dose of small area around the central axis no larger than 1 × 1 cm.

† Baseline pass rates should be established during EPID QA system commissioning and deviations in the pass rate in either direction should be monitored. For example, if an institution's baseline was 95% pass rate at (3%/2 mm), the tolerance limits should be 93–97% with ±2% tolerance and 92–98% with ±3% tolerance using the same criteria.

Table 8.

Achievable γ passing rates and dose agreement obtained from QA measurement results reported in the literature when using EPIDs for pretreatment and transit dosimetry.

2D PRE-TREATMENT TECHNIQUES

First author year	Delivery technique	Metric: γ criteria	Average gamma pass rate (%γ<1)
Howell, 2008 (Varian Portal Dosimetry)	IMRT	3%G*/3 mm	95.9±10%
Nelms 2010 (SNC EPIDose)	IMRT	3%G/3 mm	99.7±0.1% (range 94.0–100)
		2%G/2 mm	97.8±0.4% (range 82.0–100)
Bailey 2012 (EPIDose, Portal Dosimetry)	IMRT, VMAT	3%G/3 mm	>95% (range 95–99)
Wu 2012 (RadCalc EPID)	IMRT, VMAT	3%G/3 mm	IMRT: 97.2±3.0% (range 89.8–100)
			VMAT: 95.5±6.0% (range 69.3–100)

TRANSIT DOSIMETRY TECHNIQUES

First author year	Delivery technique	Anatomical site(s)	Metric	Average achieved agreement
François 2011 (EPIgray)	IMRT	Prostate	$\Delta Dose_{iso}$ †	1.6±1.4%
Ricketts 2016 (EPIgray)	3DCRT	Breast	$\Delta Dose_{iso}$, mean γ ‡	−0.6±7.4% (2SD), 0.38 (range 0.03–1.17)
	IMRT	Prostate	$\Delta Dose_{iso}$, mean γ	−4.4±8.2% (2SD), 0.80 (range 0.36–1.34)
	IMRT	H&N	$\Delta Dose_{iso}$, mean γ	−5.4±24% (2SD), 0.89 (range 0.54–1.38)
Celi 2016 (EPIgray)	3DCRT/IMRT/VMAT	Various	$\Delta Dose_{iso}$	1.9±5.2%
Cilla 2016 (SOFTDISO)	VMAT	H&N	$\Delta Dose_{iso}$	0.2±1.9%
			2D 3%G/3mm ⧫	93%; γ_{mean}: 0.42
Consorti 2017 (SOFTDISO)	SBRT	Lung	$\Delta Dose_{iso}$	±4%
			2D 3%G/3mm ◆	96%; γ_{mean}: 0.6
Piermattei. 2018 (SOFTDISO)	3DCRT/IMRT/VMAT	HN, Brain	2D 3%G/3mm	99%
		Breast, Abdomen, Thorax, Pelvis 2D	5%G/5mm	96%, 96%, 93%, 95%
Nailon 2019 (RadCalc EPID)	3DCRT/VMAT	9 sites	$\Delta Dose_{iso}$	1.9±4.5%
Sterckx 2019 (iViewDose)	VMAT	Prostate	3D 3%G/3mm	99.0±1.0% (1SD); γ_{mean}: 0.33±0.03(1SD)
Yedekci 2019 (iViewDose)	VMAT	Prostate	3D 3%G/3mm	97.2±2.6% (1SD) (range 92.7–100)

* G: Global

† $\Delta Dose_{iso}$: Dose deviation at the isocenter

‡ Mean γ: the mean gamma of the comparison

2D 3%G/3mm: 2D dose distribution in the global gamma analysis and 3mm distance to agreement

3D 3%G/3mm: 3D dose distribution in the global gamma analysis and 3mm distance to agreement

Table 9.

Metrics and tolerance limits reported in the literature when using EPIDs for PSQA.

PRE-TREATMENT TECHNIQUES				
First Author Year	**Delivery Technique**	**Anatomical Site(s)**	**Metric**	**Tolerance Limits***
van Zijtveld 2006	IMRT	Various	2D γ: 3% local/3 mm	P_{min} ($\gamma < 1$): 85%; area $\gamma > 1$: <1 cm^2
Howell 2008	IMRT	Various	2D γ: 3% local/3 mm	P_{min} ($\gamma < 1$): 89.6%; γ_{max}: 3.20; γ_{mean}: 0.47
Wu 2012	IMRT	Various	2D γ: 3% local/3 mm	P_{min} ($\gamma < 1$): 90%
Wu 2012	VMAT	Various	3D γ: 5% local/3 mm	P_{min} ($\gamma < 1$): 90%
TRANSIT DOSIMETRY TECHNIQUES				
First Author Year	**Delivery Technique**	**Anatomical Site(s)**	**Metric†**	**Tolerance Limits***
Hanson 2014	3DCRT	All, except CNS and TBI	$\Delta Dose_{iso}$	±5%
Mijnheer 2015	3DCRT/IMRT/VMAT	Most	3D γ: 3% global/3 mm/50%	P_{min} ($\gamma < 1$): 85%; γ_{max}: 2.0; γ_{mean}: 0.5; $\Delta Dose_{iso}$: ±3%
		H&N/rectum/gynecology	3D γ: 3% global/3 mm/50%	P_{min} ($\gamma < 1$): 80%; γ_{max}: 2.5; γ_{mean}: 0.7; $\Delta Dose_{iso}$: ±4%
		Breast	3D γ: 3% global/3 mm/50%	P_{min} ($\gamma < 1$): 50%; γ_{max}: 5.0; γ_{mean}: 0.5; $\Delta Dose_{iso}$: ±3%
Ricketts 2016	3DCRT	Breast	$\Delta Dose_{iso}$	±7%
	IMRT	H&N	$\Delta Dose_{iso}$	−6% ± 7%
	IMRT	Prostate	$\Delta Dose_{iso}$	−4% ± 8%
Celi 2016	3DCRT/IMRT/VMAT	Most	$\Delta Dose_{iso}$	±7.5%
		Breast—lateral	$\Delta Dose_{iso}$	±6.7%
		Int. mammary lymph nodes	$\Delta Dose_{iso}$	±10.0%
Cilla 2016	VMAT	H&N	$\Delta Dose_{iso}$	±5%
			2D γ: 3% global/3 mm	P_{min} ($\gamma < 1$): 90%; γ_{mean}: 0.67
Piermattei 2018	3DCRT/IMRT/VMAT	6 sites	$\Delta Dose_{iso}$	±5%
			2D γ: 3% global/3 mm	P_{min} ($\gamma < 1$): 90%; γ_{mean}: 0.67
Nailon 2019	3DCRT/VMAT	9 sites	$\Delta Dose_{iso}$	±10%
Bossuyt 2020	3DCRT/IMRT/VMAT	Breast	2D γ: 7% local/6 mm/ 20% threshold	P_{min} ($\gamma < 1$): 90%
		Whole brain radiotherapy	2D γ: 7% local/3 mm/ 20% threshold	P_{min} ($\gamma < 1$): 90%
		Palliative treatments	2D γ: 7% local/5 mm/ 20% threshold	P_{min} ($\gamma < 1$): 93%

PRE-TREATMENT TECHNIQUES				
First Author Year	**Delivery Technique**	**Anatomical Site(s)**	**Metric**	**Tolerance Limits***
		H&N and brain	2D γ: 3% global/3 mm/20% threshold	P_{min} (γ < 1): 95%
		Rectum	2D γ: 5% global/5 mm/20% threshold	P_{min} (γ < 1): 93%
		Other treatment sites (with mask)	2D γ: 5% global/3 mm/20% threshold	P_{min} (γ < 1): 95%
		Other treatment sites (without mask)	2D γ: 5% global/5 mm/20% threshold	P_{min} (γ < 1): 95%
		Stereotactic	2D γ: 10% local/1,2,3 mm/20% threshold	P_{min} (γ < 1): 95%

CNS = Central Nervous System; TBI = Total Body Irradiation.

*P_{min} (γ < 1): minimum pass rate; γ_{max}: maximum γ; γ_{mean}: mean γ.

†$\Delta Dose_{iso}$: dose deviation at the isocenter.

Med Phys. Author manuscript; available in PMC 2024 July 08.